

Eurasian Chemical Communications (ECC)

Volume No. 7

Issue No. 2

May- August 2025



ENRICHED PUBLICATIONS PVT. LTD

**S-9, IInd FLOOR, MLU POCKET,
MANISH ABHINAV PLAZA-II, ABOVE FEDERAL BANK,
PLOT NO-5, SECTOR-5, DWARKA, NEW DELHI, INDIA-110075,
PHONE: - + (91)-(11)-47026006**

Eurasian Chemical Communications (ECC)

Aims and Scope

Eurasian Chemical Communications (ECC) publishes experimental, theoretical and applied research papers related to all branches of Chemistry. The world of the Internet is a multi-faceted one. Each and every field of Internet is witnessing tremendous growth in the present century. But, researchers still have to wait for a long time to publish their research articles in reputed journals. To tide over this disadvantage, we have launched this online research journal.

All papers submitted to Eurasian Chem. Commun. are subjected to peer review. All contributions in the following forms are invited

SUBJECTS AREA

Related subjects:

1. Analytical Chemistry
2. Biochemistry & Biophysics
3. Inorganic Chemistry
4. Organic Chemistry
5. Physical Chemistry
6. Effects of Chemical Drugs
7. Medicinal Studies of Synthetic Drugs
8. Pharmaceutical Chemistry
9. Neurochemical Research
10. Clinical Chemistry
11. Chemical Pathology
12. Computational Chemistry
13. Mathematical chemistry

All Fields Related to Chemical Science

All papers submitted to Eurasian Chem. Commun. are subjected to peer review. All contributions in the following forms are invited

- (a) Original Research Articles
- (b) Review Articles
- (c) Short Communications

Contact Us

E-Mail: ss.sajjadifar@gmail.com (Dr. Sami Sajjadifar, Owner & Director-in-Charge)

Tel & Fax number: +98 (84) 32226101

ECC Editorial Office (Miss. Panahi): panahi.maryam406@yahoo.com

Eurasian Chemical Communications (ECC)

Editor-in-Chief

Prof. Dr. Vinod Kumar Gupta Department of Biological Sciences, Faculty of Science, King Abdulaziz University, Jeddah, Saudi Arabia Professor in Physical Chemistry, www.iitr.ac.in/departments/CY/pages/People+Faculty+vinodfcy.html , vinodfcy@iitr.ac.in 91-01332-285801	Prof. Dr. Hassan Karimi-Maleh1. Department of Applied Chemistry, University of Johannesburg, South Africa. 2. School of Resources and Environment, University of Electronic Science and Technology of China (UESTC), 611731, PR China. Professor Dr. in Nanotechnology and electrochemistry www.sre.uestc.edu.cn/info/1005/6280.htm h.karimi.maleh@gmail.com +989112540112, 0000-0002- 1027-481X
--	--

International Editorial Board

Professor Dr. Rafael Luque Universidad de Cordoba, Departamento de Quimica Organica, Campus de Rabanales, Cordoba Spain Professor of Chemistry www.uco.es/~q62alsor/Templates/profesores.html , rafael.luque@uco.es 0000-0003-4190-1916	Prof. Dr. Necip Atar Pamukkale University, Engineering Faculty, Department of Chemical Engineering, 20070, Denizli, Turkey. Professor of Electro-analytical Chemistry, Environmental Engineering, Chemical and biochemical sensors, Waste-water treatment, Fuel cells, Technical Textiles, natarpau.edu.tr +90 5079919764, 0000-0001-8779-1412
Prof. Dr. Mehmet Lütfi Yola Iskenderun Technical University, Turkey Professor of Materials Science, Analytical Chemistry, Nanotechnology, Biosensors, iste.edu.tr/person/mlutfi-yola , mehmetyolagmail.com , +90 326 613 56 00	Dr. Lucian A. Lucia Laboratory of Soft Materials & Green Chemistry, Departments of Chemistry, Forest Biomaterials, North Carolina State University, Raleigh, NC 27695, USA, Associate Professor of Soft Materials Chemistry, cnr.ncsu.edu/directory/lucian-lucia/ lalucian@ncsu.edu +1 919 515 7707 (Of 0000-0003-0157-2505)
Dr. Mohammad Mansoob Khan Chemical Sciences, Faculty of Science, Universiti Brunei Darussalam, Jalan Tungku Link, Gadong, BE 1410, Brunei Darussalam, Tanzania. Associate Professor in Inorganic Chemistry, expert.ubd.edu.bn/mansoob.khan.php , mansoob.khan@ubd.edu.bn , +673 246 0922 / 246 0000-0002-8633-7493	Dr. Amir Razmjou School of Chemical Engineering, University of New South Walse, UNSW, 2052, Sydney, Australia, Senior Research Associate in Lithium recovery, ion separation, membrane technology, nanobiosensing, www.researchgate.net/profile/Amir_Razmjou , amir@unsw.edu.au , 61-2- 9385434
Dr. Ali Maleki Department of Chemistry, Iran University of Science and Technology (IUST), Tehran 16846-13114, IRAN Associate Professor of Organic Chemistry www.iust.ac.ir/find.php?item=20.10930.19490.fa , maleki@iust.ac.ir ,	Dr. Behrooz Maleki Department of Chemistry, Hakim Sabzavari University, Sabzavar, Iran. Associate Professor of Organic Chemistry www.mendeley.com/authors/6506335669/b.maleki@hsu.ac.ir , ac.ir , +985144013324, 0000-0002-0322-6991
Professor Dr. Reza Ghiasi Department of Chemistry, East Tehran Branch, Islamic Azad University, Tehran, Iran, Professor of Inorganic Chemistry. www.scopus.com/authid/detail.uri?authorId=6507495898 , rezaghiasi135@yahoo.com , 0000-0002- 1200-6376	Prof. Dr. Ramzi MAALEJ Faculty of Sciences of Sfax (University of Sfax) 3018, Sfax- TUNISIA, Professor of Physics (Photonics, Spectroscopy and Simulation), ramzimaalej.wixsite.com/pam-group , ramzi.maalej@fss.usf.tn , 00 216 98 656 305, 0000-0002- 6722-1882

Prof. Mahmood M. Barbooti Department of Chemistry, University of Technology, Baghdad, Iraq, Professor in Analytical Chemistry www.researchgate.net/profile/Mahmood_Barbooti2 100076uotechnology.edu.iq, +964 750 241 5259 0000-0002-9793-7400	Professor Dr. M. Jamaluddin Ahmed Department of Chemistry, University of Chittagong, Chittagong-4331, Bangladesh, Professor in Analytical Chemistry and Environmental Science, Website: www.cu.ac.bd , pmjahmed55@gmail.com , +8801715001800 0000-0002-3765-066x
Professor Dr. Siyamak Shahab Head of Department of Ecological Chemistry and , Biochemistry of the International Sakharov Environmental Institute of the Belarusian State University. Professor in Physical Chemistry www.famous-scientists.ru/14673 , siyamak.shahab@yahoo.com , +375296389322	Dr. Saravanan Rajendran Faculty of Engineering, Department of Mechanical Engineering, University of Tarapacá, Avda, General Velasquez, 1775, Arica, Chile Associate Professor of Nanomaterials, materials science, photocatalyst, metal oxides, sensor www.scopus.com/authid/detail.uri?authorId=7004886581 , saravanan3.raj@gmail.com , +91900358840, 0000-0002-3771-4694
Editorial Board	
Dr. Ali Maleki Department of Chemistry, Iran University of Science and Technology (IUST), Tehran 16846-13114, IRAN Associate Professor of Organic Chemistry www.iust.ac.ir/find.php?item=20.10930.19490.fa , malekiiust.ac.ir ,	Dr. Behrooz Maleki Department of Chemistry, Hakim Sabzavari University, Sabzavar, Iran. Associate Professor of Organic Chemistry www.mendeley.com/authors/6506335669/b.malekihsu.ac.ir , +985144013324, 0000-0002-0322-6991
Professor Dr. Ali Niazi Department of Chemistry, Faculty of Science, Islamic Azad University, Central Tehran Branch, Tehran, Iran, Professor in Analytical Chemistry www.scopus.com/authid/detail.uri?authorId=7003844592 , ali.niaz@gmail.com , 0000-0002-0894-532X	Professor Dr. Reza Tayebee Department of chemistry, Hakim Sabzevari univ., Sabzevar, Iran, Professor of Nanotechnology and Biotechnology, rtayebe@yahoo.com , 0000-0003-1211-1472
Dr. Hamid Saeidian Department of Chemistry, Payame Noor University, PO BOX 19395-4697 Tehran, Iran Professor of Organic Chemistry, saeidian1980@gmail.com , 02433471217, 0000-0003-1516-9178	Dr. Gholamabbas Chehardoli Department of Medicinal Chemistry, School of Pharmacy, Hamadan University of Medical Science, Hamadan, Iran Associate Professor of Organic Chemistry cheh1002@gmail.com , +98 811 8381594
Journal staff	
Director-in-Charge	
Dr. Sami Sajjadifar	
Department of Chemistry, Payame Noor University, PO BOX 19395-4697 Tehran, Iran. Associate Professor of Organic Chemistry chemsajjadifar.blogspot.com/ , ss.sajjadi@farpnu.ac.ir , 08432226101, 0000-0001-8661-1264	
Deputy Editor	
Prof. Mohammad A. Khalilzadeh	
Department of Biomaterials, College of Natural Resources, North Carolina State University, United States, Professor in Organic Chemistry, khalilzadeh73@gmail.com	
Editorial Manager	
Professor Dr. Mohammad	
Haghighi Reactor and Catalysis Research Center, Chemical Engineering Faculty, Sahand University of Technology, P.O.Box 51335-1996, Tabriz, Iran Professor of Chemical Engineering: Nano-Catalysts, Nano Materials, Natural Gas and Carbon Dioxide Utilization, Green Fuels, Air & Water Pollution Control and Treatment, rcrc.sut.ac.ir , haghighisut.ac.ir , +98-41-33458096, 0000-0001-6683-097X	

Advisory Board

Dr. Hamid Reza Arandiyan

Senior Research Fellow at University of Sydney, Sydney, Australia, Senior Researcher in Environmental Science & Engineering www.sydney.edu.au/science/about/our-people/academic-staff/hamid-arandiyan.html, hamid.arandiyan@sydney.edu.au, 0000-0001-5633-3945

Assistant Editor

Dr. Ghobad Mansouri

Department of Chemistry, Payame Noor University (PNU), Ilam, Iran., Assistant Professor of Inorganic Chemistry www.scopus.com/authid/detail.uri?authorId=34571338200, mansouri.gh@gmail.com, 0000-0002-0589-2832

Executive Manager

Dr. Seyed Sajad Sajadikhah

Department of Chemistry, Payame Noor University, PO BOX 19395-4697 Tehran, Iran. Associate Professor of Organic Chemistry, ssajadipnu.ac.ir

Language Editor

Dr. Behroz Jamalvandillam

Farhangyan University, Ilam, Iran., University lecturer in applied linguistics, behrouzjamlvaand@gmail.com, 0000-0003-4162-2052

Mr. Ermia Aghaie

Department of Chemical and Materials Engineering, University of Alberta, Edmonton, Alberta, T6G 1H9, Canada. M.Sc. in "Materials Engineering", · www.researchgate.net/profile/Ermia_Aghaie, · ghaieualberta.ca 001-7808502047, 0000-0003-4048-8250

Editorial Manager

Maryam Panahi

Payame Noor University, maryampanahi20mpg@gmail.com
0000-0003-0149-1967

Eurasian Chemical Communications (ECC)

(Volume No. 7, Issue No. 2, May- August 2025)

Contents

Sr. No	Article/ Authors	Pg No
01	Synthesis, characterization, and evaluation of molecular docking and experimented antioxidant activity of some new chloro azetidine-2-one and diazetine-2-one derivatives from 2-phenyl-3-amino-quinazoline-4(3H)-one -Assma Abbas Alabady* Suaad M.H. Al-Majidi	1 - 18
02	Electrocatalytic hydrogenation of azobenzene and nitrocyclohexane with dispersed microparticles into alkylammonium) films - Tahar Melki* Maroua Imène Benamrani Ahmed Zouaoui	19 - 27
03	Effect of garlic extract as corrosion inhibitor for copper in acidic medium - Nawras Saad Mohamed Ramadan* Zainab Wajdi Ahmed	28 - 36
04	Study of middle graph for certain classes of graph by applying degree-based topological indices - Muhammad Shoaib Sardara,* Muhammad Asad Alia Faraha Ashrafa Murat Cancanb	37 - 50

Synthesis, characterization, and evaluation of molecular docking and experimented antioxidant activity of some new chloro azetidine-2-one and diazetine-2-one derivatives from 2-phenyl-3-amino-quinazoline-4(3H)-one

Assma Abbas Alabady* |Suaad M.H. Al-Majidi

Department of Chemistry, College of Science, University of Baghdad, Baghdad, Iraq

ABSTRACT

This research aimed to synthesize new series of β -lactam derivatives from reaction of 2-phenyl-3-amino-quinazoline-4(3H)-one (3) through several reactions. Firstly, the reaction of anthranilic acid with benzoyl chloride gives N-benzoyl anthranilic acid (1). Then, cyclization of N-benzoyl anthranilic acid with acetic anhydride to give 2-phenyl-4H-benzo[3,1]oxazine-4-one (2). After that, compound (2) was reacted with hydrazine hydrate to give 2-phenyl-3-aminoquinazoline-4(3H)-one (3). Compound (3) was reacted with different parasubstituted aromatic aldehydes to give Schiff base derivatives (49). Finally, cyclization of Schiff base derivatives with different reagents (chloroacetyl chloride, phenyl isocyanate, and phenyl isothiocyanate) to form a new four-membered heterocyclic ring (β -lactam and 1,3-diazetine-2-one (10-15) and (16-27), respectively). The prepared compounds were characterized by FTIR, $^1\text{H-NMR}$, and $^{13}\text{C-NMR}$ as well as measurements of some of its physical properties and specific tests were done. The antioxidant activity of all the prepared compounds was estimated by molecular docking studies and in an experiment.

INTRODUCTION

Quinazoline derivatives are of great importance in biological activities, such as they exhibit antitumor [1,2], diuretic [3], antiinflammatory [4,5], hypotensive [6,7], anticonvulsant [8], anti-allergy [9], depressant [10], and into-cancer properties [11]. Several selective derivatives of quinazoline containing drugs such as lapatinib, erlotinib, and vandetanib have been approved as anticancer [12] antibacterial [13]. It was also reported that drugs thioquinazoline derivatives identified as a possible pharmacophore for anti-tubercular activity [14]. Schiff bases are an important material for inorganic chemists due to their diverse biological, pharmacological, and antitumor activities. They have gained much importance in biomimetic modeling applications, molecular magnet molecules, liquid crystals aspect, and inorganic chemistry [15,16]. Polymeric Schiff bases and coordination polymers have high thermal stability, chemical resistance, scratch resistance, and corrosive resistance [17]. The β -lactam ring is a part of the core structure of several antibiotic families. β -lactam antibiotics are primarily classified as penicillin, cephalosporin, carbapenems, and monocyclic antibiotics structure [18,19].

Materials and methods

All used chemicals were purchased from Fluka Aldrich starting chemical compounds. Melting points (MP) were marked by using gallenkamp in open glass capillaries by using a Thomas capillary melting point apparatus uncorrected. FTIR spectra were recorded on SHIMAZU FTIR8400 Fourier transform infrared spectrophotometer as KBr disc. Total primary components and reagent were pure and commercially available. ^1H -NMR and ^{13}C -NMR spectra were recorded by 500 Mhz spectrometer. Dimethyl sulfoxide solvent ($\text{DMSO}-d_6$) was used to record Agilent Technologies model ultra-shield nuclear magnetic resonance (NMR) spectra, and the chemical shifts are given in δ (ppm) downfield by using tetramethylsilane (TMS) as references. UV-VIS spectra were recorded by Shimadzu-spectrophotometer and apcl PD-303-spectrophotometer, Japan. Schiff bases were synthesized as intermediate compounds, which were then treated with various reagents (chloroacetyl chloride, phenyl isocyanate, and phenyl isothiocyanate) and under various conditions to yield new heterocyclic compounds (azetidine and 1,3-diazetidine) bearing quinazoline-4(3H)-one core[15].

Synthesis of N-benzoyl anthranilic acid[20]

To the cold and stirred solution from anthranilic acid (1.37 g, 0.01 mol) dissolved in (5 mL) dry acetone, the solution of benzoyl chloride (1.16 mL, 0.01 mol) with (0.5 mL) dry pyridine was added in dropwise addition with cooling by an ice bath, the mixture was refluxed for (3 hours) in a water bath at (40-50) $^{\circ}\text{C}$, and then cooled to room temperature and poured into ice-cold diluted HCl (5%). The solid light-yellow precipitate was filtered, washed with distilled water, and recrystallized from (ethanol-water). Physical properties of compound (1) and FTIR spectral data are represented in Table 1.

Synthesis of 2-Phenyl-4H-benzo [3,1] oxazine-4-one (2) [21]

A solution of compound (1) (2 g, 0.001 mol) which dissolved in acetic anhydride (3 mL, 0.032 mol) was refluxed for (4 hours) in dry conditions. After cooling the solution to room temperature, the mixture was poured into cold petroleum ether to give crystals that were recrystallized from ethanol. Physical properties of compound (2) and FTIR spectral are demonstrated in Table 1.

Synthesis of 2-phenyl-3-amino-quinazoline 4(3H)-one (3) [22]

Compound (2) (1 g, 0.001 mol) was dissolved in (8 mL) ethanol as solvent; excess of 99% hydrazine hydrate was added to the reaction mixture and refluxed for (8 hours). Finally, the reaction mixture cooled to room temperature, poured on ice-cold water, stirred, and filtered. The precipitate was recrystallized from ethanol and water. Physical properties of compounds (3) and FTIR spectral data are indicated in Table 1. Compound (3) (0.5 g, 0.001 mol) with an equimolar amount of different para-substituted aromatic aldehydes (0.001 mol) was added, in (5 mL) absolute ethanol and (23) drops of a catalyst glacial acetic acid. The mixture was refluxed for (8-12) hours and recrystallized from ethanol and water to form base derivatives (4-9). Physical properties of compounds (4-9) and FTIR spectral data are shown in Table 2.

TABLE 1 Physical properties and FT-IR spectral data for prepared compounds (1-3)

Compound	Physical properties				FTIR absorptions spectral data cm^{-1}			
	Structure	M.P $^{\circ}\text{C}$	Yield %	Color	$\nu(\text{C-H})$ Aromatic	ν (C=O)	$\nu(\text{C=C})$ Aromatic	Other bands
1		166 - 167	75	Light yellow	3001	1710 acid 1685 amide	1544 1496	$\nu(\text{OH})$ broad 3600- 3240
2		123 - 124	85	Off white	3039	1764 lactone	1600 1573	$\nu(\text{C=N})$ 1612 $\nu(\text{C-O})$ 1257
3		169 - 170	80	White	3039	1660	1591 1560	$\nu(\text{C=N})$ 1639 $\nu(\text{NH}_2)$ asym. 3438 sym. 3309

TABLE 2 Physical properties and FT-IR spectral data cm^{-1} of prepared Schiff's base compounds (4-9)

Compound	Physical properties				FTIR absorptions spectral data cm^{-1}			
	Structure	M.P $^{\circ}\text{C}$	Yield %	Color	$\nu(\text{C-H})$ Aromatic	$\nu(\text{C=O})$ Amide	$\nu(\text{C=N})$ $\nu(\text{C=C})$	Other bands
4		240- 241	85	Yellow	3039	1681	1641 1604 1450	$\nu(\text{NO}_2)$ asym. 1558 sym. 1344 δ p-position 815 $\nu(\text{C=O})$ overtone $\nu(\text{C=O})$ 3431
5		150- 152	78	Pale Yellow	3039	1697	1641 1589 1452	$\nu(\text{C-Cl})$ 1093 δ p-position 804 $\nu(\text{C=O})$ overtone $\nu(\text{C=O})$ 3431
6		233- 225	71	White	3037	1685	1635 1583 1527	-----
7		110- 112	83	Yellow	3062	1684	1643 1515 1556	$\nu(\text{C=O})$ Overtone $\nu(\text{C=O})$ 3431 δ p-position 811

8		143-145	88	Brown	3062	1685	1650 1600 1575	ν (C=O) overtone 3427 ν (C-O-C) s.as.1251 sym.1159 δ p-position831
9		209-210	70	Yellow	3033	1680	1645 1598 1560	ν (C=O) overtone with ν O-H3425 δ p-position831

Synthesis of 3-(3-chloro-2-(4-subst. Phenyl) oxo azetidin-1-yl)-2-phenyl quinazoline-4(3H)-one (10-15) [24]

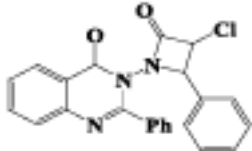
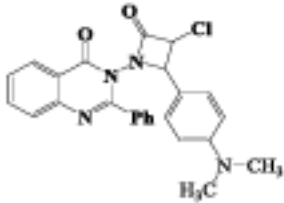
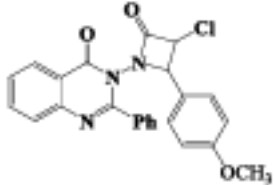
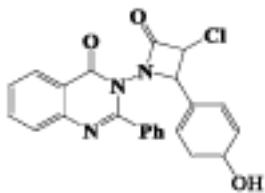
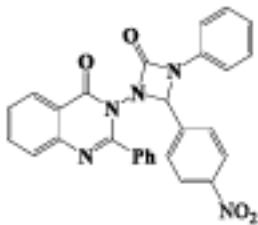
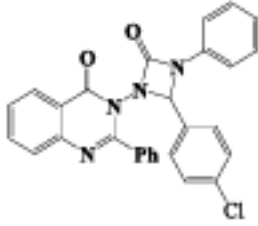
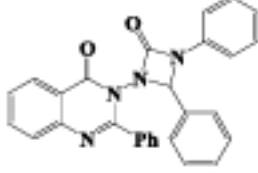
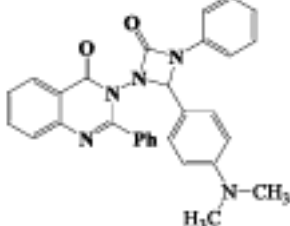
A mixture of equimolar amounts of (0.5 g, 0.001 mol) Schiff bases derivatives (3-8) in (2 mL) of dry DMF as a solvent, chloro acetyl chloride (0.2 mL, 0.001 mol), and tri ethylamine (Et₃N) (0.1 mL, 0.001 mol.) was added at (0-5)°C. The mixture was in reflux condition for (14-16) hours at (45) °C. Then, it cooled at room temperature. The products (10-15) were washed with cool water and recrystallization by using ethanol to form required products (10-15). Physical properties of compound (10-15) and FTIR spectral data are listed in Table 3.

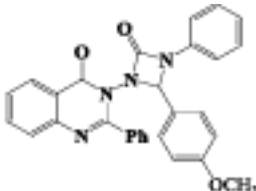
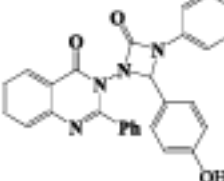
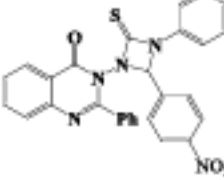
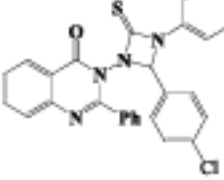
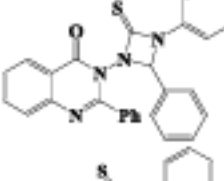
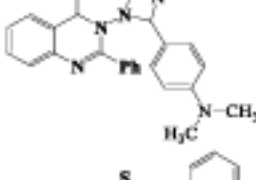
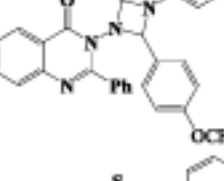
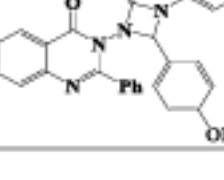
Synthesis of 3-[2-(4-subst. Phenyl)-4-oxo -3phenyl-1,3-diazetidin-1-yl]-2-phenyl quinazoline-4-(3H)-one (16-21). and 3-[2-(4sub. Phenyl)-4-thioxo-3-phenyl-1,3-diazetidin-1-yl]-2-phenyl quinazoline-4-(3H)one (22-27) [25]

A solution of (0.0016 mol) Schiff bases (4-9), phenyl isocyanate, and phenyl iso thio cyanate (0.1 mL, 0.001 mol) in (5 mL) ethanol were added in a round-bottomed flask with continuous stirring in addition to the reaction mixture was heated at room temperature, and then heated under reflux condition for (5-6) hours. The products (16-27) were washed with cool water and recrystallization by using ethanol to form the required products (16-27). Physical properties of compound (16-27) and FTIR spectral data are shown in Table 3.

TABLE 3 Physical properties of compounds (10-27)

Compound	Structures	Physical properties		
		M.p.°C	Yield %	Color
10		180-182	88	Deep brown
11		160-162	82	Pale white

12		214-216	83	White
13		236-238	80	Yellow
14		160-162	85	Peggy
15		210	70	Brown
16		118-120	83	yellow
17		236-238	75	White
18		160-162	80	White
19		164-166	85	Brown

20		212-214	78	White
21		190-192	82	Pale brown
22		230-232	83	Deep yellow
23		160-162	80	Yellow
24		130-132	82	Peggy
25		158-159	85	Brown
26		156-158	78	Brown
27		250-252	75	Pale white

Antioxidant activity (DPPH radical scavenging assay)[26]

The antioxidant activity of compounds (3-27) was assessed by using the stable DPPH free radical according to a known procedure. A variety of concentrations of (50,100, and 150) mg/mL of the synthesized compounds (3-27) were mixed with methanol solution (up to 3 mL) including 0.0001

mg/mL of DPPH radical. The absorbance of the reaction mixture was measured at 517 nm after incubation for 30 min at room temperature by using a spectrophotometer. Ascorbic was used as the positive control at the concentrations of the tested compounds. Percentage inhibitions of compounds (3-27) and that of ascorbic acid were calculated by using the following formula:

$$\text{DPPH inhibition effect (\%)} = ((\text{Ac}-\text{As})/\text{Ac}) * 100$$

Ac=Absorbance reading of the control

As=Absorbance reading of the sample

In silico studies Ligand preparation Molecular docking studies were performed with Small Drug Discovery Suites package (Schrodinger 2020-3, LLC). Two dimensional structures of the synthesized compounds were sketched, and then converted into 3D structures by using the LigPrep module in maestro 12.5. To prepare ligands for the docking process, the ligands were set to the physiological pH and by using the OPLS-2005 force field performed energy minimization. The epik option was used for keeping the ligand in the correct protonation state.

Protein processing and binding site identification

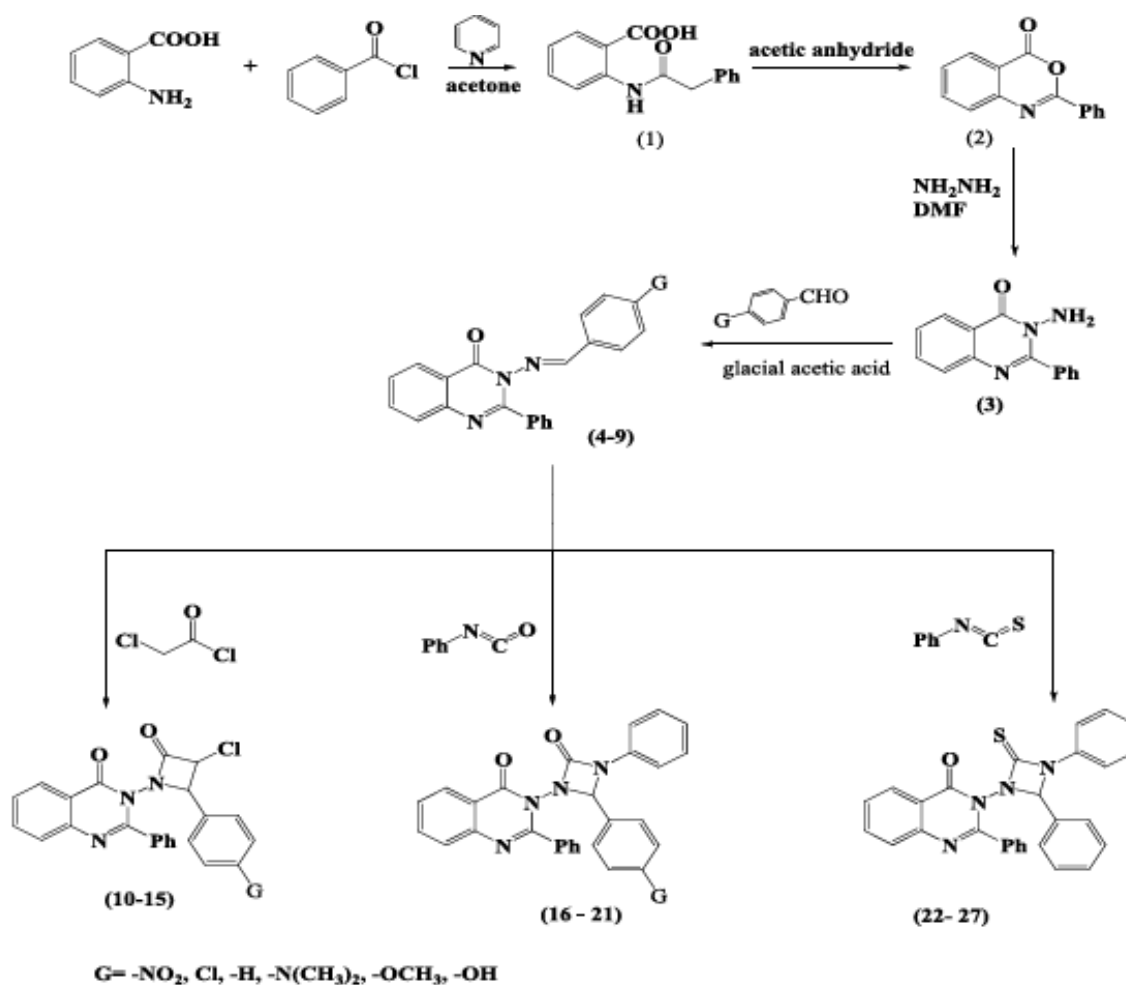
The 3D crystal structures of the (3-27) enzyme were obtained from RCSB Protein Data Bank (PDB ID: 3pp0). The 3D crystal structure was repaired and prepared via protein preparation wizard in maestro 12.5. All water molecules were initially removed from the crystal structure. Bond orders and charges were assigned, and then all missing hydrogen atoms were added to the protein structure. Amino acids were ionized by setting physiological pH byPropka software. Finally, the restrained minimization step has also been performed by using the OPLC force field. This minimized structure was the best structure to utilize for molecular docking. After protein potential preparation, top-ranked protein binding sites were identified to determine the most suitable binding site of proteins by using the glide grid tool of maestro 12.5.

Results and discussion

The series of the reactions that were carried out to prepare the new chloro azetidine-2-one,1,3-diazetiden-2-one,and 1,3diazetidne 2- thione quinazoline derivative -4(3H)-one displayed in Scheme 1.

The FTIR spectrum for compound (1) indicated characteristic broad absorption bands at $\nu(3600-3240)\text{cm}^{-1}$ due to $\nu(\text{OH})$, $(3396)\text{cm}^{-1}$ for $\nu(\text{N-H})$, $(3001)\text{cm}^{-1}$ due to $\nu(\text{C-H})$ aromatic, and two bands that appeared at $(1710)\text{cm}^{-1}$ and $(1685)\text{cm}^{-1}$ belonged to $\nu(\text{C=O acid})$ and $\nu(\text{C=O amide})$, respectively, also, at $(1544,1496)\text{cm}^{-1}$ for $\nu(\text{C=C})$ aromatic. Compound(2) was prepared by cyclization reaction of compound (1) in the presences of anhydride. Disappearing bands of carbonyl group of amid NH group of compound (1) in the FTIR spectrum of compound (2) was a good evidence for the formation of this compound (2). Conversion of compound (2) into 2-phenyl-3-amino-quinazoline-4(3H)one compound (3) was performed in the presences of hydrazine hydrate. The FTIR spectrum of this compound showed a strong absorption band at (asys. 3438 and sym. $3309)\text{cm}^{-1}$ for (NH_2) group and $(3039)\text{cm}^{-1}$

due to $\nu(\text{C-H})$ aromatic, (1660) cm^{-1} for stretching band due to (C=O amide). While $^1\text{H-NMR}$ spectrum of compound (3) is depicted in Table 5, $^{13}\text{C-NMR}$ spectrum data of this compound (3) demonstrated in Table 5, it was subjected to condensation reaction with para-substituted aromatic aldehydes to form Schiff bases derivatives (4-9). The FTIR spectra of these compounds showed absorption bands at -1635-1650) cm^{-1} due to $\nu(\text{C=N})$. $^1\text{H-NMR}$ spectrum of compound (7) was shown in Table 5. $^{13}\text{C-NMR}$ spectra data of these compounds (7 and 8) were listed in Table 5. Schiff base derivatives (4-9) were subjected to cyclization reaction with different reagents (chloro acetyl chloride, phenyl isocyanate and phenyl iso thio cyanate) to form 4-oxoazetidin derivatives (10-15), 4-oxo-1,3-diazetidin derivatives (16-21) and 4-thioxo-1,3-diazetidin derivatives (22-27), respectively.



SCHEME 1 Synthesis of compounds (10-27)

The FTIR spectra (Table 3) of 4-oxoazetidin derivatives (10-15) revealed new bands at (1658-1701) cm^{-1} owing to (C=O lactam ring). $^1\text{H-NMR}$ spectra were depicted in Table 6; $^{13}\text{C-NMR}$ spectra data of these compounds (13 and 15) was listed in Table 5. presented in Table 6; $^{13}\text{C-NMR}$ spectra data of these compounds (19,20) was listed in Table 5.

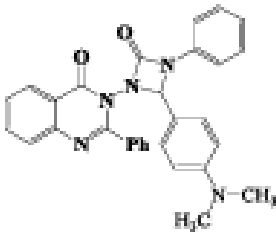
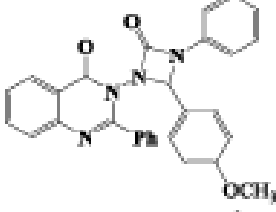
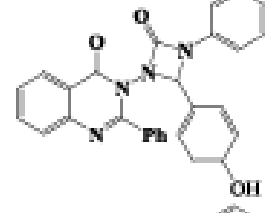
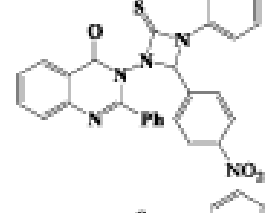
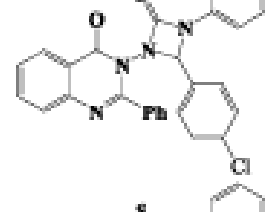
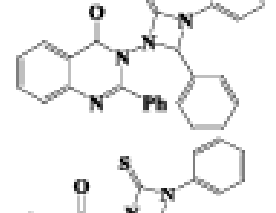
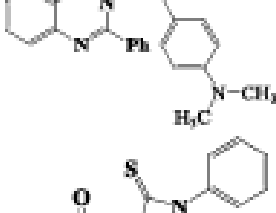
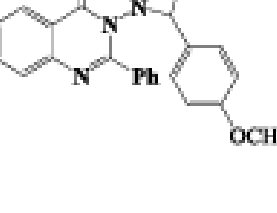
The FTIR spectra of 4-oxo-1,3-diazetidin derivatives (16-21) illustrated bands at (1668-1699) cm^{-1} for (C=O lactam). $^1\text{H-NMR}$ spectra of compounds (19, 20) were The FTIR spectra (Table 3) of 4-thioxo-1,3diazetidin derivatives (22-27) showed new bands at (1438-1477) cm^{-1} for (C=S) group. $^1\text{H-NMR}$ spectra of compounds (22-27) were illustrated in Table 6. $^{13}\text{C-NMR}$ spectra data of these compounds

(19,20) was listed in Table 5.

The FTIR spectra (Table 3) of 4-thioxo-1,3diazetidin derivatives (22-27) showed new bands at (1438-1477) cm^{-1} for (C=S) group. ^1H -NMR spectra of compounds (22-27) were illustrated in Table 6. ^{13}C -NMR spectra data of these compounds (22 and 27) was listed in Table 4.

TABLE 4 FTIR spectral data cm^{-1} of compounds (10-27)

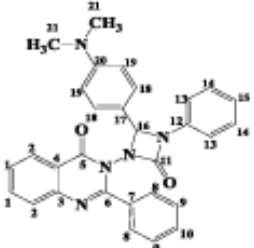
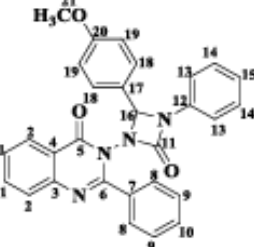
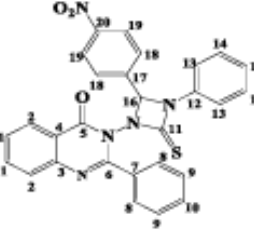
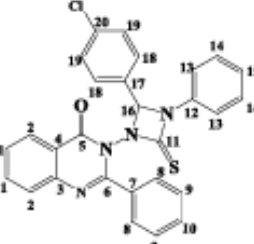
No.	Structures	$\nu(\text{C-H})$ Arom.	Major FTIR Absorption cm^{-1}		
			$\nu(\text{C=O})$	$\nu(\text{C=C})$ Arom.	Other bands
10		3001	1679 lactam 1649 quinazoline	1573 1475	$\nu(\text{NO}_2)$ asym. 1573 sym. 1342 $\delta\text{p-position}$ 802 $\nu(\text{C-Cl})$ 923
11		3068	1683 lactam 1649 quinazoline	1556 1475	$\nu(\text{C-Cl})$ 923 $\delta\text{p-position}$ 761
12		3039	1680 lactam 1651 quinazoline	1558 1477	$\nu(\text{C-Cl})$ 923
13		3065	1683 Lactam 1651 quinazoline	1591 1477	$\delta\text{p-position}$ 806 $\nu(\text{C-Cl})$ 923
14		3055	1683 lactam 1652 quinazoline	1577 1492	$\delta\text{p-position}$ 825 $\nu(\text{C-Cl})$ 921
15		3064	1680 Lactam 1650 quinazoline	1554 1475	$\nu(\text{OH})$ 3433 $\nu(\text{C-Cl})$ 921 $\delta\text{p-position}$ 831
16		3060	1686 lactam 1650 quinazoline	1539 1442	$\nu(\text{NO}_2)$ asym. 1539 and sym. 1317 $\delta\text{p-position}$ 827
17		3055	1683 lactam 1654 quinazoline	1577 1450	$\nu(\text{C-Cl})$ 1014 $\delta\text{p-position}$ 825
18		3056	1686 lactam 1649 quinazoline	1577 1442	

19		3047	1679 Lactam 1653 quinazoline	1565 1445	$\nu(\text{aliph. CH})$ 2981, 2804 $\delta p\text{-position}$ 815
20		3001	1679 lactam 1650 quinazoline	1573 1475	$\delta p\text{-position}$ 802
21		3062	1680 lactam 1650 quinazoline	1583 1448	$\nu(\text{OH})$ 3463 $\delta p\text{-position}$ 827 $\nu(\text{C-O})$ 1276
22		3058	1680 Lactam 1652 quinazoline	1575 1448	$\nu(\text{C=S})$ 1448, $\nu(\text{NO}_2)$ asym. 1519 sym. 1338 $\delta p\text{-position}$ 831
23		3058	1683 Lactam 1652 quinazoline	1591 1494	$\nu(\text{C=S})$ 1450 $\delta p\text{-position}$ 825 $\nu(\text{C-Cl})$ 1091
24		3050	1683 Lactam 1650 quinazoline	1589 1413	$\nu(\text{C=S})$ 1452
25		3065	1685 Lactam 1650 quinazoline	1591 1494	$\nu(\text{C=S})$ 1444 $\delta p\text{-position}$ 815
26		3055	1683 Lactam 1654 quinazoline	1591 1492	$\nu(\text{C=S})$ 1448 $\delta p\text{-position}$ 806

27		3029	1683 Lactam 1654 quinazoline	1556 1477	$\nu(\text{OH})$ 3444 $\nu(\text{C}=\text{S})$ 1413 δp -position 825
----	--	------	---------------------------------------	--------------	--

TABLE 5 ^1H -NMR and ^{13}C -NMR spectral data (δ ppm) compounds (3, 7, 8, 13, 15, 19, 20, 22, and 23)

Compound	Structure	^1H -NMR spectral data (δ ppm)	^{13}C -NMR spectral data (δ ppm)
3		3.37(s, 2H, NH_2); 7.21-8.73(m, 9H, Ar-H)	117.41 (C10); 120.31 (C2); 127.39 (C4); 128.27 (C8); 128.53 (C7); 129.48 (C9); 130.49 (C1); 146.72 (C3); 156.86 (C6); 167.78 (C5).
7		3.47(s, 6H, $\text{N}-(\text{CH}_3)_2$); 6.67(s, 1H, $\text{N}=\text{CH}-$); 8.32-8.60 (m, 13H, Ar-H);	40.50 (C16); 121.27 - 139.74 (C3, C4, C7, C12); 127.48-129.21 (C1, C2, C8, C9, C10, C13); 150.57 (C15); 152.18 (C6, C11); 164.96 (C5).
8		3.38 (s, 3H, OCH_3); 7.35(s, 1H, $\text{N}=\text{CH}-$); 7.37-8.58 (m, 13H, Ar-H);	40.06 (C16); 120.90-129.50 (C1, C2, C8, C9, C10, C13); 132.16- 140.37 (C3, C4, C7, C12); 143.81 (C15); 151.47 (C6, C11); 165.38 (C5).
13		2.98(d, 1H, CH-Cl azetidine ring); 3.04 (s, 6H, $\text{N}(\text{CH}_3)_2$); 3.35 (s, 1H, CH diazetidin ring); ; 6.75-8.62(m, 13H, Ar-H).	43.01(C18); 63.11(C12); 65.31 (C13); 150.55-121.61(C1, C2, C3, C4, C7, C8, C9, C10, C14, C15 , C16, C17); 152.19 (C6); 164.91(C5) ; 168.91 (C11).
15		2.88(d, 1H, CH-Cl azetidin ring); 3.36(s, 1H, CH di azetidine ring); 6.85-8.8 (m, 13H, Ar-H), 10.34 (s, 1H, OH).	60 (C12); 70(C13); 128.11- 116.24 (C1, C2, C3, C4, C7, C8, C9, C10, C14, C15, C16, C17); 153.61(C6); 165.16 (C5); 169.99(C11).

19		3.38(s,6H,2CH ₃); 4.14(s,1H,CH di azetidine ring); 6.75-8.71 (m,17H,Ar-H).	40.59(C21); 60.56(C16); C12(60);140.19-121.61 (C1,C2,C3,C4,C7,C8,C9, C10,C13,C14,C15,C17, C18,C19,C20);154.01(C6);1616 0.29(C5);164.92 (C11).
20		3.35(s,3H,CH ₃) ; 4.13 (s,1H, CH di azetidine ring); 6.98-8.59 (m,18H,Ar-H).	52.42(C21);60.55(C16);140.35-118.6 (C1,C2,C3,C4,C7,C8,C9,C10,C12, C13,C14,C15,C17,C18, C19,C20);154(C6);164.92(C5), 165.38(C11).
22		3.37(s,1H, CH di azetidine ring);7.14-8.56(m,18H,Ar-H).	67.16(C16);140.79-121.07 (C1,C2 C3,C4,C7,C8,C9,C10,C12,C13,C1 4,C15,C17,C18,C19, C20);148.47 (C6);165.7 (C11); 165.08(C5).
23		3.36(s,1H,CH diazetidine ring);7.15-8.72 (m,18H,Ar-H).	65.31(C16);139.78-120.97 (C1,C2,C3,C4,C7,C8,C9, C10,C12,C13,C14,C15, C17,C18,C19,C20);148.13 (C6);165.5(C5);166.93 (C11).

Antioxidant activity

Antioxidants can stop the oxidative stress by binding with free radicals and neutralizing their harmful effects through several chemical mechanisms created by natural active [26]. Oxidative degradation of organic materials, including biological molecules such as lipids, proteins, foods, and cosmetics, like any other radical chain reaction, autoxidation is composed of three steps: initiation, propagation, and termination [27].

DPPH scavenging activity

All the compounds (3-27) and starting 2phenyl-3-amino-quinazoline-4(3H)-one showed comparable or slight less activity than the standard (ascorbic acid). It was predestined by DPPH (2,2- diphenyl-1picrylhydrazyl) assay method at various concentrations (50,100, and 150 µg/mL). The result depending on the reaction characterized by a change in its deep violet color (DPPH) or Decolourization is stoichiometric concerning several captured electrons. Compounds (3-27) exhibited the best results among all compounds. Some compounds (4, 11, 17, and 22) bearing a nitro group (electron-withdrawing group) at a para-position showed high antioxidant activity when compared with some

compounds (8, 14, 20, and 26) that have methoxylgroup (electron-donating group).

Compounds (5, 11, 17, and 23) substituted with halogen groups-Cl (electronwithdrawing group) exhibits a good antioxidant activity. These Compounds (6, 8, 12, 14, and 20) appear to be the antioxidant activity that is decreased. These compounds possessed good reducing power ability at a concentration of (150 $\mu\text{g/mL}$) among other compounds and exhibited close or higher antioxidant activity than the standard solution (ascorbic acid). Figure 1 displays the DPPH scavenging activity of the newly synthesized compound, as shown in Table 7.

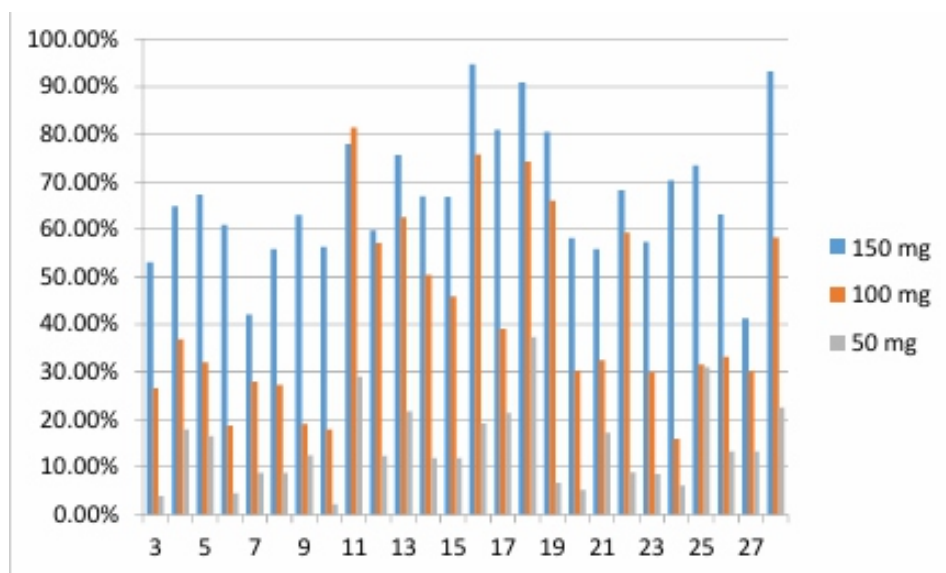


FIGURE 1 DPPH scavenging activity of the newly synthesized compound

Total antioxidant capacity

The total antioxidant capacity of the synthesized compounds was evaluated by the phosphomolybdenum method. A different concentrations (50, 100, and 150 mg/mL) of an aliquot compound solutions was combined with (1 mL) of reagent (0.6 M) sulfuric acid, (28 mM) sodium phosphate, and (4 mM) ammonium molybdate. All containing the reaction solution for the tested compounds were capped and incubated at 95 °C for 90 min. Next, the tubes were cooled to room temperature, and then the absorbance of each tube was measured by using a spectrophotometer at 695 nm against blank. The total antioxidant activity is expressed as the number of grams equivalent to ascorbic acid. Different concentrations (10, 20, 30, 50, 70, 90, 120, 180, and 200 $\mu\text{g/mL}$) of ascorbic acid with DW where it is used to plot the calibration curve, as depicted in Figure 2.

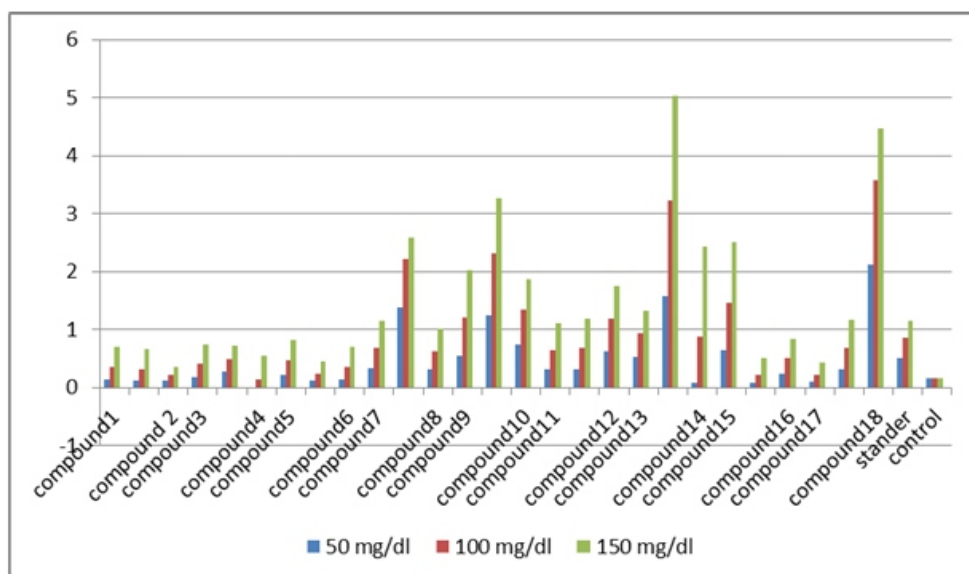


FIGURE 2 Total antioxidant capacity for compound

Molecular docking studies [28]

Ligand docking was performed for the prediction of the best poses and binding energies of ligands at binding sites identified by glide grid tool on the receptor. All ligands were initially docked on the receptors by using Glide docking module in Maestro 12.5. Briefly, grid box was generated around the selected co-crystallized ligand at the binding site by using the receptor grid generation platform. Then rigid receptor docking simulations were performed by the extra precision options in maestro 12.5. both visualizing poses and results analyses were performed by using maestro 12.5 space visualizer, as illustrated in Figure 2.

TABLE 6 The molecular docking of compounds (1-22)

Compound	Types of residues	Types of interaction	Docking score	Glide Energy	Glidersmsd	Glideposenum
2		Hydrophobic	-7.63096	-50.3906	32.8306	2
3	MET 801	Hydrophobic	-7.61815	-47.646	33.48688	4
4		Hydrophobic	-7.35403	-34.7349	34.87986	3
5	ASP 808	Hydrophobic	-7.18914	-45.9591	32.63256	10
6		Hydrophobic	-6.80809	-43.9367	33.45379	2
7		polar	-5.85965	-38.1529	34.99858	1
8	LYS 753	polar	-5.83351	-44.4437	33.14897	9
9	ARG 849	Charge positive	-4.40299	-23.9661	34.99762	3
10		Charge positive, negative	-2.74401	-41.2674	33.18349	2
	ARG 849	H-bond				
11	ARG 811	Pi-cation	-2.61187	-41.8032	34.10098	28
	SER728	Halogen bond				
12	ASP 863	Hydrophobic	-2.02553	-34.5091	33.28576	9
13	-----	Charge negative	-1.94687	-34.3469	33.50194	7
14	Glycin	Charge negative	-1.93338	-33.672	33.25601	24
15	SER 728	H-bond	-1.88123	-36.547	32.80697	1
16			-1.74724	-39.0748	33.46274	3

17	----- -	Hydrophobic	-1.68242	-28.7082	32.75414	2
18		Hydrophobic	-1.50985	-33.9516	33.51797	3
19	LYS 724	Pi-cation	-1.37096	-29.4818	33.02363	1
20	ARG 849	Hydrophobic	-1.04894	-31.8322	33.69674	10
21	CYS 805	Hydrophobic	-0.77708	-24.1768	32.04859	15
22	ARG 849	Hydrophobic	-0.77708	-24.1768	32.32675	15
	CYS 805	H-bond	-0.33853	-32.8685	32.7587	1

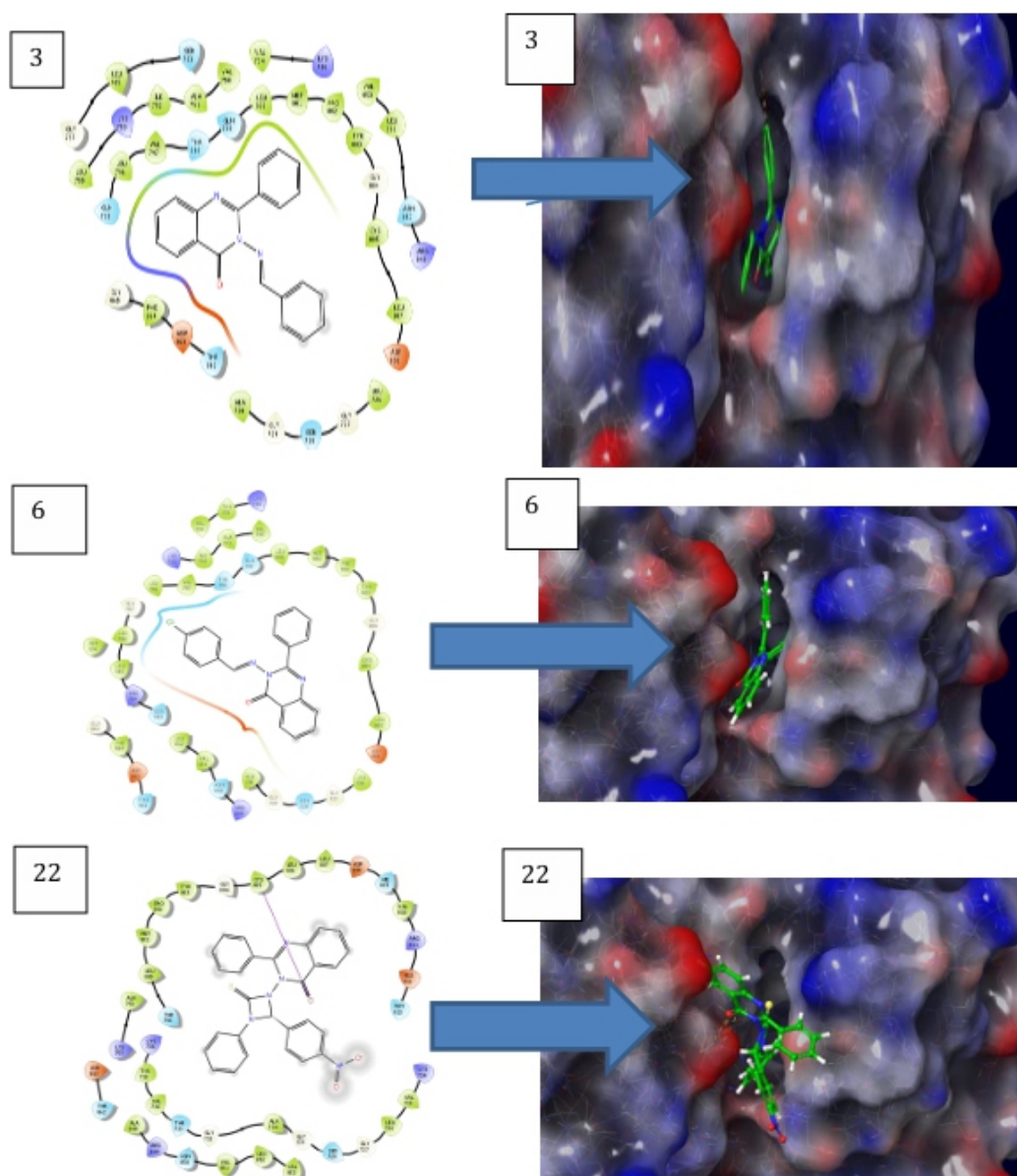


FIGURE 3 The best and stable conformations of all the synthesized molecules

The best result was related to compounds (1, 2, 3, and 4) for docking score ranging from [(-7.630)-(-7.189)] and RMSD score ranging from (32.8306- 32.7587), as indicated in Figure 3.

The compounds (5, 6, 7, and 8) for docking scores range from ranging from [(-6.80809)(-4.402)] and RMSD score ranging from (33.45379-34.99762) as showed in Figure 3. On other hand, the lowest results for compounds (9-22) for docking score ranging from [(-2.744)-(0.338)] and RMSD score ranging from (33.18349-32.7587), as demonstrated in Figure 3.

The docking was perfect for compounds (1-4).the best interaction was with the target protein for compound (2). The type of residues was (MET) at (801) where a type of interaction was (hydrophobic). This combination gives the best grove pose and affinity for the protein, this situation was shown in less form for the compounds (5-8) as the residue (LYS) at (753), (ARG) at (849), and type of interaction was (polar).

The situation was less appropriate for compounds (5-8) because this compound have lower interaction with the target protein. For compound (6), the types of residues and the type of interaction (polar). This combination gives the lower grove pose and affinity for the protein. Finally, the worst result was for compounds (9-22). This gives less interaction with the target protein, this may be for the reasonthat the residues and interaction were very weak as it has (CYS) at position (805) with (Hbond) interaction, this gives a low affinity and makes interaction as nearly impossible. According to this results we can state that this value can give a good prediction for the protein-compound interaction, this prediction will consume less time and our results show the best compound is can be used for laboratory experiment and gives us the desired effect without using any form of compounds (9-22) that will consume our efforts.

Conclusion

Various derivatives of new β -lactam were synthesized from Schiff bases derivatives and different reagents (chloro acetyl chloride, phenyl isocyanate, and phenyl isothiocyanate). These derivatives were identified with FT-IR, ¹HNMR, ¹³CNMR, and physical properties. All synthesized derivatives were studied in-vitro antioxidant activity. The results revealed a good biological property. We used molecular docking and chemical synthesis to study the structure activity relationships of compounds as inhibitors for TEM-class β lactamase.

In the last study [29],new β -lactams were synthesized from N-carbazole derivatives. Physical and chemical properties and identified for all synthesized compounds of (tetra hydro carbazole and N-carbazole) derivatives and they studied in-vitro antioxidant activity for compounds. The results showed that a test had been a good ant-biological activity. In this study, we evaluated synthesized, molecular characterized, docking, and of some new chloro azetidine-2-one and diazepine-2-one derivatives from 2-phenyl-3-amino-quinazoline-4(3H)-one in addition to newly application for this group from organic compounds.

Acknowledgements

I extend my thanks and appreciation to my esteemed professor (Prof. Dr. Suad Mohamed Hussein) for suggesting the topic of the research to supervise it and for the effort she made and the valuable advice

and guidance she provided, hoping that God would preserve her as an asset to support the scientific process.

Conflict of Interest

The authors declare that there is no conflict of interests regarding the publication of this manuscript.

Orcid:

Assma Abbas Alabady: <https://www.orcid.org/0000-0001-88823017>

References

- [1] H.S. Abulkhair, *Al-Azhar J. Pharm. Sci.*, 2021, 64, 69-79. [Crossref], [Google Scholar], [Publisher]
- [2] M.A. Hawata, W.A. El-Sayed, E.S. Nossier, A.A.H. Abdel-Rahman, *Biointerface Res. Appl. Chem.*, 2022, 12, 5217-5233. [Crossref], [Google Scholar], [Publisher]
- [3] M.U. Rahman, A. Rathore, A.A. Siddiqui, G. Parveen, M. SYar, *J. Enzyme Inhib. Med. Chem.*, 2014, 29, 733-743. [Crossref], [Google Scholar], [Publisher]
- [4] M.C. Raghu, C.B. Pradeep Kumar, K.Y. Kumar, M. Prashanth, B. Jayanna, *J. Heterocycl. Chem.*, 2019, 56, 2046-2051. [Crossref], [Google Scholar], [Publisher]
- [5] M.F. Zayed, M.H. Hassan, *Saudi Pharm. J.*, 2014, 22, 157-162. [Crossref], [Google Scholar], [Publisher]
- [6] R.S. Pathak, V. Malhotra, R. Nath, K. Shanker, *Cent. Nerv. Syst. Agents Med. Chem.*, 2014, 14, 34-38. [Crossref], [Google Scholar], [Publisher]
- [7] A.D. Khalaji, M. Ghorbani, *Chem. Methodol.*, 2020, 4, 532-542. [Crossref], [Google Scholar], [Publisher]
- [8] E. Jafari, M.R. Khajouei, F. Hassanzadeh, G.H. Hakimelahi, G.A. Khodarahmi, *Res. Pharm. Sci.*, 2016, 11, 1-14. [Pdf], [Google Scholar], [Publisher]
- [9] P.S. Chaudhari, S.S. Chitlange, R.K. Nanda, *Antiinflam Antiallergy Agents Me Chem.*, 2018, 17, 102-114. [Crossref], [Google Scholar], [Publisher]
- [10] S. Verma, A.S. Pathania, S. Baranwal, P. Kumar, *Lett. Drug Des. Discov.*, 2020, 17, 1552-1565. [Crossref], [Google Scholar], [Publisher]
- [11] M. Szewc, E. Radzikowska-Büchner, P. Wdowiak, J. Kozak, P. Kuszta, E. Niezabitowska, M. Masłyk, *Int. J. Mol. Sci.*, 2022, 23, 2745. [Crossref], [Google Scholar], [Publisher]
- [12] A.S. Alqahtani, M.M. Ghorab, F.A. Nasr, M.Z. Ahmed, A.A. Al-Mishari, S.M. Attia, *Molecules*, 2022, 27, 981. [Crossref], [Google Scholar], [Publisher]
- [13] A.D. Khalaji, M. Emami, N. Mohammadi, *J. Med. Chem. Sci.*, 2021, 4, 626-634. [Crossref], [Google Scholar], [Publisher]
- [14] A.A. Shanty, J.E. Philip, E.J. Sneha, M.R.P. Kurup, S. Balachandran, P.V. Mohanan, *Bioorg. Chem.*, 2017, 70, 67-73. [Crossref], [Google Scholar], [Publisher]
- [15] A.D. Khalaji, *Chem. Methodol.*, 2020, 4, 34-39. [Crossref], [Publisher] [Google Scholar],
- [16] Y. Ding, Z. Li, C. Xu, W. Qin, Q. Wu, X. Wang, W. Huang, *Angew. Chem.*, 2021, 133, 24-40. [Crossref], [Publisher] [Google Scholar],
- [17] D. Nartop, E. Tokmak, E.H. Özkan, H.E. Kızıl, H. Ögütçü, G. Ağar, S. Allı, *J. Med. Chem. Sci.*, 2020, 3, 363-372. [Crossref], [Google Scholar], [Publisher]

-
- [18] S.F. Ayad, S.M. Mahmood, A.A. Mohamed, *Best International Journal of Humanities, Arts, Medicine and Sciences*, 2014, 2, 67-78. [Google Scholar], [Publisher]
- [19] S.M. Al-Majidi, H.M. Al-tamimy, *IOSR J. Appl. Chem.*, 2017, 10, 37-46. [Crossref], [Google Scholar], [Publisher]
- [20] H.M. Al-tamimy, S.M.H. Al-Majidi, *IOSR J. Appl. Chem.*, 2016, 9, 36-44. [Crossref], [Google Scholar], [Publisher]
- [21] A.S. El-Azab, S.G. Abdel-Hamde, M.M. Sayed-Ahmed, G.S. Hassan, T.M. El-Hadiyah, O.A. Al-Shabanah, H.I. El-Subbagh, *Med. Chem. Res.*, 2012, 22, 2815-2827. [Crossref], [Google Scholar], [Publisher]
- [22] S.M. Al-Majidi, H.J. Al-Adhami, *Baghdad Sci. J.*, 2016, 13, 345-359. [Crossref], [Google Scholar], [Publisher]
- [23] P.S. Sankar, K. Divya, G.D. Reddy, V. Padmavathi, G.V. Zyryanov, *AIP Conference Proceedings*, 2019, 2063, 040047. [Crossref], [Google Scholar], [Publisher]
- [24] A.W. Naser, A.M. Majeed, *J. Chem. Pharm. Res.*, 2015, 7, 300-306. [Google Scholar], [Publisher]
- [25] R. Muhiebes, E.O. Al-Tamimi, *Chem. Methodol.*, 2021, 5, 416-421. [Crossref], [Google Scholar], [Pdf]
- [26] L. Valgimigli, A. Baschieri, R. Amorati, *J. Mater. Chem. B*, 2018, 6, 2036-51. [Crossref], [Google Scholar], [Publisher]
- [27] P. Ahmad, H. Woo, K.Y. Jun, H.A. Abdel-Aziz, Y. Kwon, A.F.M. Motiur Rahman, *Bioorg. Med. Chem.*, 2016, 24, 18981908. [Crossref], [Google Scholar], [Publisher]
- [28] S.M. Al-Majidi, Z.M. Al-Mohson, T.H. Mathkor, *Journal Connect.*, 2021, 21, 09761772. [Crossref], [Google Scholar], [Publisher]
-

Electrocatalytic hydrogenation of azobenzene and nitrocyclohexane with dispersed copper microparticles into poly (pyrrole - alkylammonium) films

Tahar Melki* | Maroua Imène Benamrani | Ahmed Zouaoui

ABSTRACT

This paper presents the results of the electrocatalytic hydrogenation of azobenzene and nitrocyclohexane on carbon felt cathodes modified by poly(pyrrole-alkylammonium) films and containing dispersed metallic copper microparticles in a hydroorganic medium at neutral and basic pH. The effect of the polymers' structures, the cathode nature, and the effect of synthesis methods on the electrocatalytic activity of the electrodes have been examined, as well. The obtained products were identified by gas chromatography in comparison with authentic ones. It is found that azobenzene leads to aniline, while nitrocyclohexane to cyclohexanone oxime. Indeed, these cathodes allow the hydrogenation of the substrates at potentials between -1 and -1.2 V/SCE in basic medium and between -0.65 and 0.85 V/SCE in neutral medium, lower as compared with their reduction potentials. It is indicated that the best chemical and electrical yields are obtained in a basic medium and the chemical yields of the formed products increase with the amount of copper inserted, while the length of the alkylammonium chain has no remarkable influence on yields. It has been demonstrated that these cathodes have a good electrocatalytic activity despite the very small amount of copper inserted into the polymer film.

KEYWORDS Electrocatalytic hydrogenation; modified poly(pyrrole-alkylammonium); nitro-compounds.

INTRODUCTION

The initial investigation on electrocatalytic hydrogenation goes back at the beginning of the 20th century [1-3]. This was forgotten for sometimes due to the low activity of the utilized cathodes, often made of bulk transition metals. Electrocatalytic hydrogenation can be likened to the conventional catalytic hydrogenation. However, this method has important advantages:

- The use of hydrogen generated in situ rather than from an external source; its production can therefore be controlled by adjusting the potential or the current density; place
- The electrocatalytic hydrogenation can take at lower pressures and temperatures because hydrogen is generated in an already activated form;
- In comparison with the conventional electroreduction techniques, electrocatalytic hydrogenation makes it possible to achieve reductions at less negative potentials, which makes it possible to orient the reduction differently, to decline energy consumption, and to avoid the formation of by-products [4].

Due to its low cost, catalytic activity and interesting selectivity, nickel has been used in the electrocatalytic hydrogenation of organic compounds, either in the form of electrodeposited nickel on various conductive substrates or in the form of Raney nickel [5-8]. On the other hand, the use of copper in electrocatalytic hydrogenation remains limited to a few experiments carried out with electrodes based on Devarda copper [9-10] or polycrystalline copper [11-12]. In the meanwhile, nitrobenzene, phenylhydroxylamine, azoxybenzene, azobenzene, and hydrazobenzene have been reduced to aniline. In addition, the Devarda copper cathode allows to reduce nitro aliphatic compounds, such as nitrocyclohexane into cyclohexylamine [9]. Other electrodes have further been used for the electrocatalytic reduction of nitroarenes and nitrocyclohexane [13-18]. Recently, cyclohexanone oxime has been synthesized by liquid phase hydrogenation of nitrocyclohexane using a bimetallic catalyst [19]. Likewise, the recent development electrodes for the degradation of dyes [20-22], the electrochemical of CO₂ [23], as an sensor [24-25] and photoacoustic response of organic compounds is of high significance [26-27].

The dispersion of microparticles in conductive polymer films provides effective cathodes for the electrocatalytic hydrogenation of organic compounds due to the formation of chemisorbed (active) hydrogen on the surface of the electrode. The initial electrodes modified by polymer films containing noble metal particles for the electrocatalytic hydrogenation of organic compounds were developed in France at the laboratory of organic electrochemistry and redox photochemistry [28]. It has been shown that the incorporation of particles of noble metals and transition metals in films of poly (pyrrole-viologen) and polypyrrole alkylammonium, makes it possible to manufacture modified electrodes effective for the electrocatalytic hydrogenation of a number of organic functions in hydroorganic medium (water-alcohol) [28-32].

In this work, the electrocatalytic activity of carbon felt cathodes were studied which were modified by a film of polypyrrole alkylammonium containing dispersed copper microparticles for the hydrogenation of azobenzene and nitrocyclohexane in environment of water-ethanol at neutral and basic pH. The length of the carbon chain of polypyrrole substituted by alkylammonium with 3 carbons (poly1) and 12 carbons (poly2) and the method of copper insertion by exchange-reduction as well as the direct reduction were investigated.

Experimental

Instrumentation

The electrochemical equipment consisted of an EGG PAR 273 potentiostat/galvanostat. The reference electrode was either the system Ag/Ag⁺ 10⁻² M consisting of a silver wire immersed in a solution of 10⁻² M AgNO₃ in 0.1 M acetonitrile in TEAP for the study in acetonitrile, or a saturated calomel electrode with KCl (SCE), Tacussel C10, equipped with an electrolytic bridge.

Chemicals

The used reagents, electrolytes, and solvents were commercial products used without prior purification. The monomers (3-pyrrol-1-ylpropyl) triethylammonium [33], denoted 1, and (11-pyrrol-1-yl dodecyl) triethylammonium [34-35], denoted as 2, were synthesized at the Department of Molecular Chemistry,

University Joseph Fourier Grenoble (France).

Electrodes elaboration

The preparation of the modified electrodes for the preparative electrolysis is carried out in a Metrohm cell of 50 ml volume without barriers, where the auxiliary electrode is a cylindrical platinum grid placed around the working electrode. The latter having the dimension $25 \times 20 \times 4 \text{ mm}^3$ were carbon felts (RVC 2000, 65 mg cm^{-3} , Le Carbone, Lorraine) with an active electrochemical surface area of 42.5 cm^2 per cm^3 of felt [36]. These were modified by polymer films containing copper microparticles.

After depositing the polymer film by electrochemical oxidation of the monomer at 0.9 V in 0.1 M acetonitrile medium in TEAP on the carbon electrode, the incorporation of metallic copper particles into poly1 and poly2 films was carried out according to two manners, as given in the schematic diagram of Figure 1. The first manner consists of a simple immersion of the modified electrode in an aqueous solution of CuSO_4 and $\text{Na}_2\text{C}_2\text{O}_4$. Then, the anions $(\text{Cu}(\text{Ox})_2)_2^{2-}$ exchange with the counter ions Cl^- initially present in the film, and thus an electrochemical reduction at the potential of -0.5 V/SCE in an aqueous medium makes it possible to precipitate the metallic copper in the polymer film (Way A). The second manner consists of a direct electrochemical reduction of the modified electrode in an aqueous solution of CuSO_4 and $\text{Na}_2\text{C}_2\text{O}_4$, without going through independent ion exchange step (Way B).

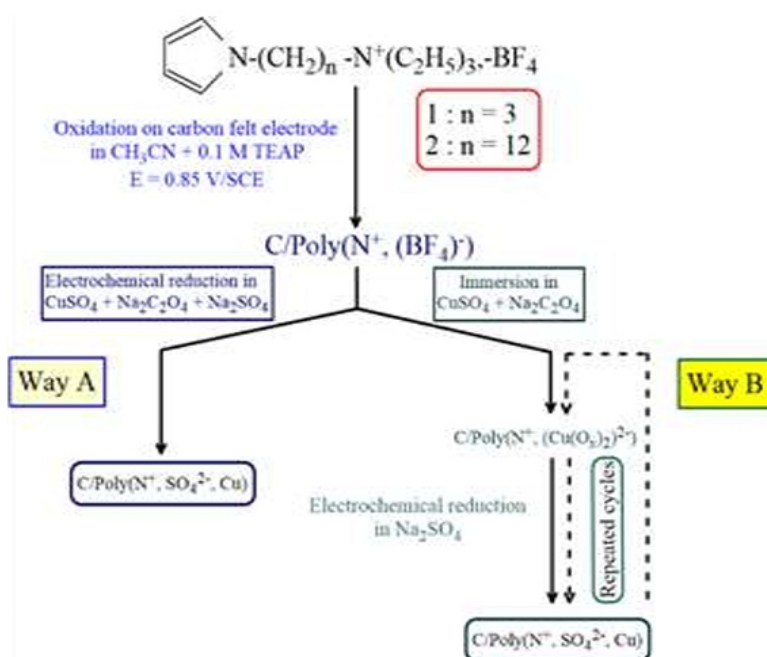


FIGURE 1 Schematic diagram of the two ways of preparing the electrode C/PolyN⁺-Cu. Way A: Direct electrochemical reduction; Way B: Reduction after an exchange procedure

The characterization of polymer-metal composites has already been presented in details in previous work. This technique makes it possible to insert the metal in the form of microparticles dispersed uniformly in the polymer film. The amount of introduced not exceeding a few micrograms [28-32,37].

Electrocatalysis

The electrolysis of azobenzene and nitrocyclohexane were carried out according to the experimental conditions described by Lessard et al. [10-11]. These were carried out in a three-compartment H-shaped cell. The modified carbon felt electrodes were placed in the cathode compartment containing 40 ml of the electrolyte. The potential was maintained between -1.0 and -1.2 V/SCE in basic solutions, and between -0.85 and -0.65 V/SCE in neutral ones. After 30 minutes of (hydrogen evolution), 1 mM of substrate was introduced into the cathode compartment. The electrolyzes were stopped after the current fell to a few mA. The end products were extracted with diethyl ether. Their identification was based on gas – chromatography (GC) in comparison with authentic samples and confirmed by GC – mass spectrometry experiments.

Chromatography analysis

The qualitative and quantitative analyzes of the electroreduction products were carried out using a Shimadzu GC-14A chromatograph equipped with a flame ionization detector and connected to a Merck D 2000 recorderintegrator. The doses were thereafter performed by comparison with authentic samples. The column (diameter 2 mm, length 3m) was filled with the phase SE 30 phase at 10% on Chromosorb W washed with acids (45/60 mesh) and sieved at 0.1 mm.

Results and discussion

Electrocatalytic hydrogenation of azobenzene During the nitrobenzene reduction to aniline, Zouaoui et al. [31] have reported the formation of azobenzene with variable yields depended on the utilized electrode and the medium pH.

With the electrodes prepared by incorporation of copper microparticles in films of poly1 or poly2, the chemical yields of azobenzene are very low due to the high catalytic activity of these cathodes, which allows the preferential reduction of nitrobenzene to aniline. On the other hand, on the electrodes of felt of bare carbon or modified by the copper deposit, the chemical yields of azobenzene are relatively high.

According to the literature, the reduction to 4 electrons of azobenzene should lead to aniline, hydrazobenzene being formed (Figure 2) [38]. The intermediate product of this reduction is hydrazobenzene and a side product is benzidine. We are therefore interested in the reduction of this compound on carbon felt cathodes modified by poly1 or poly2 films and containing copper microparticles and on bare carbon felt electrodes. The results are presented in Table 1.

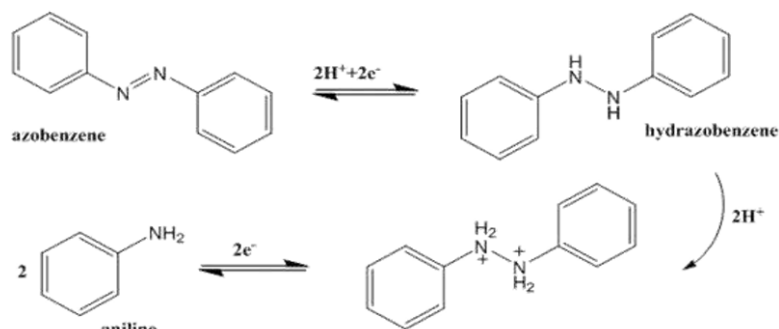


FIGURE 2 Schematic diagram of azobenzene reduction

should be noted that the cyclohexanone oxime is obtained by tautomerization of nitrocyclohexane. The most significant results obtained on the reduction of nitrocyclohexane on carbon felt cathodes modified by poly1 and poly2 films containing copper microparticles and on copper plates are presented in Table 2

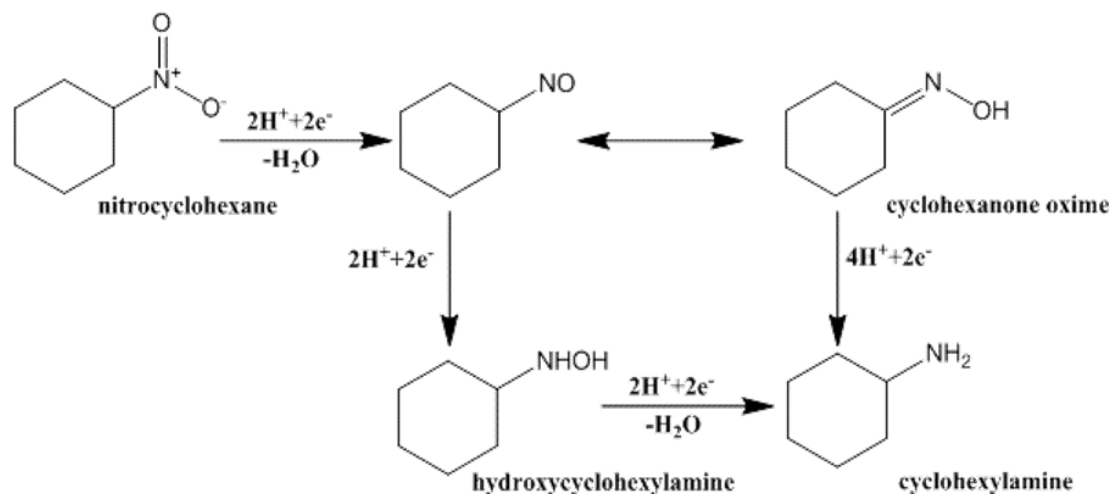


FIGURE 3 Schematic diagram of nitrocyclohexane reduction

The reduction current of nitrocyclohexane is lower than that of nitrobenzene, even at more negative potentials (- 1.1 V/SCE in basic medium and - 0.9 V/SCE in neutral one). The oxime has been the product essentially which was formed, with often quantitative chemical yields (100%, input 1). In some cases, small amounts of amine were formed (inputs 2 to 6). The non-identified by-products were further detected by gas – chromatography (inputs 5 and 6), nevertheless, hydroxylamine was not detected.

In view of the reported results in Table 2, there is no significant difference in the catalytic activity between the different electrodes, whatever the polymer (poly1 or poly2) and the incorporation manner (ion exchange-reduction or direct reduction). It is worth noting that the highest reduction currents were obtained, in the basic medium (input 3) and in the neutral one (input 5), with the electrodes prepared by direct electroprecipitation of a large quantity of copper (4 Coulombs). However, the largest amounts of cyclohexylamine (11% and 13%; inputs 2 and 4) were obtained with electrodes prepared by the ion-reduction exchange procedure. This result reveals that this manner leads to electrodes whose catalytic activity is significantly better, probably due to a more homogeneous dispersion of copper microparticles in the polymer.

The reduction of nitrocyclohexane in a basic electrolyte to the corresponding oxime on the copper plates is quite effective (input 6), however, this requires the application of a much more negative potential (- 1.5 V/SCE instead of - 1.2 V/SCE) and the resulting amount of formed amine is low (4%). In this case, the electrocatalytic activity of copper microparticles as dispersed in the films of poly1 and poly2 is further greater than that of copper plates. These cathodes are, however, less efficient than those based on copper from Devarda, which led to reduce nitrocyclohexane to cyclohexylamine with good chemical and electrical yields [9].

TABLE 1 Azobenzene electrocatalytic hydrogenation

Input	Cathode	Medium	E (V/SCE)	I_0 (mA)	I_f (mA)	Load (C)	Chemical efficiency ^b (%) PhNH ₂	Electrical efficiency ^b (%) PhNH ₂
1	C/Poly1 (1,5×10 ⁻⁵ mol) ^c -Cu (4 exchanges)	Basic	-1	25	1,2	200	36	72
2	C/Poly1 (1,2×10 ⁻⁵ mol) ^c -Cu (1 exchange)	Basic	-1	16	4	430	19	17
3	C/Poly2 (1,1×10 ⁻⁵ mol) ^c -Cu (4 exchanges)	Basic	-1	100	2,5	245	24	38
4	C/Poly1 (0,6×10 ⁻⁵ mol) ^c -Cu (1 exchange)	Neutral	-0.65	13	1,8	210	19	36
5	C/Poly2 (2,2×10 ⁻⁵ mol) ^c -Cu (4 exchanges)	Neutral	-0.65	65	3	240	35	58
6	Carbone ^d	Basic	-1	14	5,8	336	e	e
7	Carbone ^d	Neutral	-0.65	25	1	195	21	41

In basic electrolytes ($E_{app} = -1$ V/SCE) and in neutral electrolytes ($E_{app} = -0.65$ V/SCE), the electrolysis was stopped after the exchange of about 4 electrons, or after the current dropping to a few mA. Load charges varied between 200 to 430 F, corresponding to approximately 2 to 4 electrons per azobenzene molecule. The only product has been aniline with fairly good chemical and electrical yields (inputs 1 and 5). Hydrazobenzene was never detected at the end of the reactions.

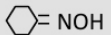
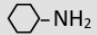
For the same polymer, the amount of incorporated copper had a significant effect on the electrocatalytic activity of the cathodes. In fact, on an electrode prepared with 4 incorporations of copper in poly1, the chemical yield of aniline is clearly greater (36%, input 1) than with a cathode prepared with a single incorporation (19%, input 2). Furthermore, the amount polymer on carbon felt had an important influence on the activity of these cathodes. The comparison between the results of inputs 1 to 5 illustrates that the production of aniline is greater in cases of thicker polymer films. This result is not surprising, since more copper particles are incorporated as the polymer film thickness is increased.

It is worth noting that the reduction of azobenzene on bare carbon felt does not take place at -1 V/SCE in a basic medium (input 6). On the other hand, in a neutral medium and at $E_{app} = -0.65$ V/SCE, aniline is formed, with a chemical yield (21%, input 7), which markedly lower than that obtained with carbon/polymer-copper cathodes under the best conditions (35%, input 5). Finally, it had been indicated that the reduction of azobenzene on a polycrystalline copper electrode leads only to hydrazobenzene [11]. All of these results once again illustrate the good electrocatalytic activity of these cathodes prepared by the dispersion of copper microparticles in polymer films.

Electrocatalytic nitrocyclohexane of hydrogenation

In comparison with that of nitroaromatic compounds, the electrochemical reduction of nitroaliphatics to their corresponding amines is more difficult. The intermediate reactions formed during the reduction process such as oxime and hydroxylamine are more stable. The reaction mechanisms of their electrochemical reduction, taking nitrocyclohexane as an example, is depicted in Figure 3 [9, 39]. It

TABLE 2 Nitrocyclohexane electrocatalytic hydrogenation

Input	Cathode	Medium	E (V/SCE)	I_0 (mA)	I_f (mA)	Load (C)	Chemical efficiency ^b (%)	
							 =NOH	 -NH ₂
1	C/Poly1 (1,2×10 ⁻⁵ mol) ^{c, d} Cu (1 exchange)	Basic	-1,1	6	1,5	180 ^g	100	-
2	C/Poly2 (2,2×10 ⁻⁵ mol) ^{c, d} Cu (4 exchanges)	Basic	-1,2	9	1,8	320	89	11
3	C/Poly1 (4,2×10 ⁻⁵ mol) ^{c, e} -Cu (2×10 ⁻⁵ mol)	Basic	-1,2	12	10	300	95	5
4	C/Poly2 (2,2×10 ⁻⁵ mol) ^{c, d} -Cu (4 exchanges)	Neutral	-0,9	19	1,6	430	87	13
5	C/Poly1 (4,2×10 ⁻⁵ mol) ^{c, d} /Cu (2×10 ⁻⁵ mole)	Neutral	-0,85	30	2	430	82	6
6	Copper Plate ^f	Basic	-1,5	25	25	600	90	4

Conclusion

This study allowed us to study the electrocatalytic activity of the modified electrodes (carbon felt/polypyrrolealkylammonium-copper) vis-à-vis the hydrogenation of azobenzene and nitrocyclohexane in water-ethanol medium at neutral and basic pH. Aniline and oxime were obtained in quantitative yields. It is important to note that, despite the very low amounts of copper contained in the polymer films, these cathodes are effective for the electrocatalytic reduction of nitrates. The amount of the metal incorporated has a great influence on the electrocatalytic activity of these modified electrodes, as demonstrated by reduction studies of azobenzene. However, we did not observe an influence of the nature of the polymer and of the incorporation manner (ion exchange-reduction or direct reduction of copper complexes) on the activity of these cathodes. Finally, although they are less efficient than the copper-based ones from Devarda, these modified electrodes are more active than the polycrystalline electrodes.

To sum up, in the case of nitrocyclohexane, the best result is obtained with the electrode modified with poly1 containing copper particles inserted by the exchange-reduction method in a basic medium. Electrocatalytic hydrogenation is selective and results only in cyclohexanone oxime with a chemical yield of 100%.

Finally, the results obtained clearly reveal that the electrocatalytic hydrogenation of the studied nitro proves to be selective.

Acknowledgments

The authors acknowledge the support from the Directorate-General for Scientific Research and Technological Development (DGRSDT-Algeria).

Conflict of Interest

The authors declare that there is no conflict of interests regarding the publication of this manuscript.

Orcid:

Tahar Melki: <https://www.orcid.org/0000-0003-3140-393X>

References

- [1] S. Fokin, *Z. Elektrochem.*, 1906, 12, 749-762. [crossref], [Google Scholar], [Publisher]
- [2] M.P. Breteau, *Bull. Soc. Chim. Fr. Ser.*, 1911, 4, 764-772.
- [3] F. Fichter, R. Stocker, *Chem. Ber.*, 1914, 47, 2003-2019. [Google Scholar], [Publisher]
- [4] A. Vélin-Prikidánovics, J. Lessard, *J. Appl. Electrochem.*, 1990, 20, 527-528. [crossref], [Google Scholar], [Publisher]
- [5] J.C. Moutet, *Org. Prep. Proc. Int.*, 1992, 24, 309-325. [crossref], [Google Scholar], [Publisher]
- [6] J.M. Chapuzet, A.N.D.R.Z.E.J. Lasia, J.E.A.N. Lessard, *Electrocatalysis*, 1998, 155-159. [Google Scholar], [Publisher]
- [7] B. Sakurai, T. Arai, *Bull. Chem. Soc. Jpn.*, 1955, 28, 93-94. [crossref], [Google Scholar], [Publisher]
- [8] D. Robin, M. Comtois, A. Martel, R. Lemieux, A.K. Cheong, G. Belot, J. Lessard, *Can. J. Chem.*, 1990, 68, 1218-1227. [crossref], [Google Scholar], [Publisher]
- [9] G. Belot, S. Desjardins, J. Lessard, *Tetrahedron Lett.*, 1984, 25, 5347-5350. [crossref], [Google Scholar], [Publisher]
- [10] A. Cyr, P. Huot, G. Belot, J. Lessard, *Electrochim. Acta*, 1990, 35, 147-152. [crossref], [Google Scholar], [Publisher]
- [11] A. Cyr, P. Huot, J.F. Marcoux, G. Belot, E. Laviron, J. Lessard, *Electrochim. Acta*, 1989, 34, 439-445. [crossref], [Google Scholar], [Publisher]
- [12] A. Martel, A.K. Cheong, J. Lessard, Brossar, *Can. J. Chem.*, 1994, 72, 2353-2360. [crossref], [Google Scholar], [Publisher]
- [13] J. Song, Z.F. Huang, L. Pan, K. Li, X. Zhang, L. Wang, J.J. Zou, *Appl. Catal. B-Environ.*, 2018, 227, 386-408. [crossref], [Google Scholar], [Publisher]
- [14] Y. Huang, J. Lessard, *Electroanalysis*, 2016, 28, 1-13. [crossref], [Google Scholar], [Publisher]
- [15] Z. Chen, Z. Wang, D. Wu, L. Ma, *J. Hazard. Mater.*, 2011, 97, 424-429. [crossref], [Google Scholar], [Publisher]
- [16] A. Ahmadi, T. Wu, *Chem. Eng. J.*, 2019, 374, 1241-1252. [crossref], [Google Scholar], [Publisher]
- [17] H.G. Liao, Y.J. Xiao, H.K. Zhang, P.L. Liu, K.Y. You, C. Wei, H. Luo, *Catal. Commun.*, 2012, 19, 80-84. [crossref], [Google Scholar], [Publisher]
- [18] K. Shimizu, T. Yamamoto, Y. Tai, A. Satsuma, *J. Mol. Catal. A Chem.*, 2011, 345, 5459. [crossref], [Google Scholar], [Publisher]
- [19] F. Yao, S. Liu, H. Cui, Y. Lv, Y. Zhang, P. Liu, F. Hao, W. Xiong, H. Luo, *ACS Sustain. Chem. Eng.*, 2021, 9, 3300-3315. [crossref], [Google Scholar], [Publisher]
- [20] R. Mohammadzadeh Kakhki, R. Tayebee, S. Hedayat, *Appl. Organometal Chem.*, 2017, 32, e4033. [crossref], [Google Scholar], [Publisher]
- [21] Tayebee R., Mohammadzadeh Kakhki R., Audebert P., Amini M.M., Salehi M., Mahdizadeh Ghohe N., Mandanipour V., Karimipour G.R., *Appl. Organometal Chem.*, 2018, 32, e4391. [crossref], [Google Scholar], [Publisher]

- [22] R. Tayebee, E. Esmaeili, B. Maleki, A. Khoshniat, M. Chahkandi, N. Mollania, *J. Mol. Liq.*, 2020, 317, 113928 [crossref], [Google Scholar], [Publisher]
- [23] P. Amos, H. Louis, K. Adesina Adegoke, E.A. Eno, A.O. Udochukwu, T. Odey Magub, *Asian J. Nanosci. Mater.*, 2018, 1, 183-224. [crossref], [Google Scholar], [Publisher]
- [24] M. Ebrahimi, H. Beitollahi, *Chem. Methodol.*, 2021, 5, 397-406. [crossref], [Google Scholar], [Publisher]
- [25] S. Salari, H. Beitollahi. *Chem. Methodol.*, 2021, 5, 407-415. [crossref], [Google Scholar], [Publisher]
- [26] M. Esmaeili, E. Koushki, R. Tayebee, A. Ghasedi, *Opt. Mater.*, 2020, 101, 109715. [crossref], [Google Scholar], [Publisher]
- [27] E. Koushki, R. Tayebee, M. Esmaeili, *J. Appl. Phys. B*, 2020, 126, 36. [crossref], [Google Scholar], [Publisher]
- [28] L. Coche, J.C. Moutet, *J. Am. Chem. Soc.*, 1987, 109, 6887-6889. [crossref], [Google Scholar], [Publisher]
- [29] I.M. F. De Oliveira, J.-C. Moutet, S. HamarThibault, *J. Mater. Chem.*, 1992, 2, 167-173. [crossref], [Google Scholar], [Publisher]
- [30] L. Coche, B. Ehui, D. Limosin, J.C. Moutet, *J. Org. Chem.*, 1990, 55, 5905-5910. [crossref], [Google Scholar], [Publisher]
- [31] A. Zouaoui, O. Stephan, M. Carrier, J.C. Moutet, *J. Electroanal. Chem.*, 1999, 474, 113122. [crossref], [Google Scholar], [Publisher]
- [32] A. Zouaoui, O. Stephan, A. Ourari, J.C. Moutet, *Electrochim. Acta*, 2000, 46, 49-58. [crossref], [Google Scholar], [Publisher]
- [33] S. Cosnier, A. Deronzier, J.-C. Moutet, J.F. Roland, *J. Electroanal. Chem.*, 1989, 271, 6981. [crossref], [Google Scholar], [Publisher]
- [34] L. Coche-Guerente, A. Deronzier, B. Galland, P. Labbe, J.C. Moutet, G. Reverdy, *J. Chem. Soc. Chem. Commun.*, 1991, 386-388. [crossref], [Google Scholar], [Publisher]
- [35] L. Coche-Guerente, A. Deronzier, B. Galland, J.-C. Moutet, P. Labbe, G. Reverdy, Y. Chevallier, *J. Amhrar, Langmuir*, 1994, 10, 602-610. [crossref], [Google Scholar], [Publisher]
- [36] L. Coche, J.C. Moutet, *J. Electroanal. Chem.*, 1987, 224, 111-122. [crossref], [Google Scholar], [Publisher]
- [37] N. Hakimi, A. Zouaoui, F. Z. Satour, A. Sahari, A. Zegadi, *J. Inorg. Organomet. Polym. Mater.*, 2020, 30, 330-336. [crossref], [Google Scholar], [Publisher]
- [38] L. Holleck, S. Vavřicka, M. Heyrovsky, *Electrochim. Acta*, 1970, 15, 645-656. [crossref], [Google Scholar], [Publisher]
- [39] M. Heyrovsky, S. Vavřicka, *J. Electroanal. Chem.*, 1970, 28, 409-420. [crossref], [Google Scholar], [Publisher]

Effect of garlic extract as corrosion inhibitor for copper in acidic medium

Nawras Saad Mohamed Ramadan* |Zainab Wajdi Ahmed
Department of Chemistry College of Education for
Pure Sciences, Ibn–AL-Haitham University of Baghdad, Baghdad, Iraq

ABSTRACT

The inhibitive effect of garlic extract on copper alloy corrosion in HNO₃ acid solutions were studied by using weight loss methods. According to the findings, the extract was effective and very good inhibitors in the acidic media. In this study, the temperature influence was investigated on the efficacy in which there is (no) extract, and finally thermodynamic activation and adsorption parameters were determined. The results of every method used in this study showed a good agreement, We utilized the Langmuir adsorption isotherm to fit experimental data and the obtained adsorption Gibb's free energy values and signs indicated the spontaneous adsorption of inhibitor molecules on copper surfaces by the mechanism of physical adsorption.

KEYWORDS Garlic extract; copper inhibition; weight loss; thermodynamic parameters; Langmuir.

INTRODUCTION

Corrosion naturally occurs affecting our life degradation to domestic gadgets and airplanes, distribution systems public roads, automobiles, and bridges [1]. Its key cause in metals is their tendency for reaching stable states. Many metal alloys are not stable and require interaction with the surrounding to obtain minor energies by the formation of the metal complexes [2].

The corruptions of the copper and copper alloys happen oxides layers (patina) are formed. Yet, these patinas degrade if exposed to polluted atmosphere [3]. Still, chemical inhibitor utilization like the chromate, nitrate, carbonate, phosphate, silicate, and other toxic compounds as an inhibitor of corrosion control confirmed their active inhibitors at relatively cheap costs, while these chemicals make additional obstacles not offering solutions [4].

Plant extracts are interesting because the corrosion inhibitors for relatively longer periods appeared from the data in review papers. In particular, natural inhibitors are particularly interesting as they seem to be environmentally friendly, readily accessible, at low costs, with renewable supply sources [5–13]. The natural-happening substance includes many organic compounds which natural like ascorbic acid, flavonoids, and pigments. Their extracts are nitrogen, compounds in sulfur and oxygen making them active anti-corrosion inhibitors. In general, an inhibitor consists of heterogeneous atoms like (N, O, and S) possessing electronic densities which suit acting as antidotes to corrosion. N, O, and S are the adsorption active center on the metal after the inhibitor of the competences of P>S>N>O [14].

Garlic is vegetable with a bulb of the family Liliaceae and is commonly distributed worldwide and China is the leader with about 81% of world. It is one of the significant preventive herbs, a spice, and a well-trusted remedy in different epidemics like dysentery, typhoid, cholera, and influenza. It is a remedy different ailment. Garlic has at least 100 sulphur-containing compounds basically to medicinal applications. Allicin is 70 to 80 % of the total thiosulphinates in it. Its smell is slight and imperceptible until peeled. Upon peeling, slicing or crushing, it at once spread intense smell with sulphur glycosides. Several studies revealed that allicin is a significant garlic element responsible for its odours, flavor and its biological features.

Although it is high medicinal and culinary values, garlic has anti-nutrition like flavonoids, saponins, tannins, alkaloids, steroids, hydrocyanide, and anthocyanin. Flavonoids, saponins and tannin of the garlic are in 0.04 to 0.36%, 0.14 to 19.0%, and 0.06 to 6.10%, respectively [15]. In this article, the new environmentally friendly corrosion inhibitor effects (garlic extract) like corrosion inhibitors to copper in nitric acid solutions were studied by the methods of the weight loss.

Experimental

Materials

The utilized copper sheet has a purity of >99.% (supplied by Local Market in Iraq). This sheet cut the samples (dimensions= 2 cm diameter= 0.5 cm). It is also mechanically polished with grade emery papers 220, 400, and 600. In addition, it is washed exhaustively with distilled water, while washing with ethanol and acetone to degrease it, and then it was stored in desiccator prior to their uses in corrosion examinations.

Sample collection and preparation

Garlic was taken from Local Market in Iraq. Distilled water was used to clean and wash it, and then it was dried at room temperatures and grounded to be powdered. Then, it was stored in the dark within containers of glasses for additional used (50 g) of it. It was put after drying in 500 mL round bottomed flasks with a 400 mL of 0.5M HNO₃ and refluxed for 1 hour in boiling degrees. Next, it was left to cool at room temperatures out of the light. The mixture was filtered with filter papers at various concentrations (200, 250, 300, 350, and 400) ppm of stock solution

Quantification of all alkaloids, saponins, and flavonoids content in the garlic extracts

Garlic powder and quantification chemical compositions of all .alkaloids, saponins, and flavonoids were made based on the standards (Fajemileh in Samuel Oladipo chemical compositions, phytochemical, and mineral profiles of garlic (*Allium sativum*), 2018 [15].

TABLE 1 Percentage compositions of chemical compounds in garlic powders

Garlic Phytochemical	Composition
Alkaloids mg/100g	4.21
Tannins mg/100g	3.54
Carotenoids mg/100g	0.64
Sappnine mg/100g	0.80
Flavonids mg/100g	5.56
Steroids mg/100g	0.04

The weight loss approaches the easiest to study corrosion inhibitors because devices (except for the use of the digital scale) are needed. This approach has the weight metal sample differences of the measured pre- and post-exposing the corrosion media (with and without inhibitors). This work weighed copper specimens completely immersing it in 0.5 M HNO₃ solutions with no (control samples) and with the garlic extract. In terms of specimens, they were circular copper foils (dimensions: 2 cm diameter and 0.2 cm thickness). We conducted these at various concentrations of garlic extract: (200, 250, 300, 350, and 400) ppm. All weight-loss calculations re-occurred three times followed by the comparison of the results. The test lasted 2 hours in stirred settings at 25 °C (298 K) in the acid media by using a new fresh solution in all experiments.

The inhibition competence (%IE), surface coverage values (θ), and corrosion rates were measured as follow:

$$\%IE = [(CR_o - CR_i) / CR_o] \times 100\% \quad (1)$$

$$\theta = (CR_o - CR_i) / CR_o \quad (2)$$

$$CR(mdd) = (w_o - w_i) / A \times t \quad (3)$$

Where, w_o and w_i are copper weight losses in mg with and without inhibitors, respectively, (θ), is the surface coverage of inhibitors; A in the outer layer areas of the copper specimens (in dm²), and t is immersion times (in days)[16].

Results and discussion

Concentration and temperature influence The inhibition efficiency differences were resulted due to the weight losses in other inhibitor concentrations in 0.5 M HNO₃ at variable temperatures (298, 308, 318, and 328K) appear in Table 2.

TABLE 2 Corrosion rates and inhibition efficiency values in two-hour immersions at various temperatures for copper in 0.5M HNO₃ with and without concentrations of garlic extracts

Temp.(K)	C _{inh} .(ppm)	CRmdd	θ	IE%
298	Blank	43.16	-	-
	200	20.22	0.53	53.00
	250	13.68	0.68	68.29
	300	11.8	0.72	72.60
	350	7.43	0.82	82.90
	400	5.21	0.87	87.90
308	Blank	47.37	-	-
	200	24.21	0.48	48.88
	250	20	0.57	57.78
	300	17.88	0.62	62.26
	350	15.54	0.67	67.19
	400	12.63	0.73	73.33
318	Blank	53.68	-	-
	200	36.84	0.31	31.37
	250	28.42	0.47	47.06
	300	24.96	0.53	53.50
	350	21.34	0.60	60.23
	400	17.89	0.66	66.77
328	Blank	70.53	-	-
	200	49.47	0.29	29.85
	250	43.15	0.38	38.80
	300	39.65	0.43	43.77
	350	29.74	0.57	57.82
	400	25.26	0.64	64.18

Based on the results, the inhibition efficiency IE% increases when concentration of the inhibitors rises and is declined by the reduction of temperatures at the same inhibitor concentrations, the inhibition efficiency showed an inverse proportion to the temperatures in which highest efficiency reached 87.9% at (298) K [18] because the adsorption amounts and the inhibitor molecule coverage on copper outer layers rises with the inhibitor concentrations, so copper surfaces are professionally drifted from the medium decrease in inhibition efficiencies with rise of temperatures suggesting adsorption mechanism[17,18].

Copper corrosion activating energy:

The activating energy measurements are for the corrosion coppers in nitric acids with (without) no garlic extract that are evaluated from Arrhenius Equation [19,20]:

$$\log i_{\text{corr}} = \frac{-E_a}{2.303RT} + \log A \quad (4)$$

Where, (E_a) and (R) are the activating energy is the gas constant, respectively (8.314), while (A) refers to the Arrhenius constant. According to Equation 4, plotting $\log (i_{\text{corr}})$ versus $\frac{1}{T}$ should appear linear as we practically noticed line slopes giving $\frac{-E^*}{RT}$, yet the line intercept extrapolated to $\frac{1}{T} = 0$ giving $\ln A$

By using alternative relationships (ΔH) and (ΔS):

$$\ln \left(\frac{i_{\text{corr}}}{T} \right) = \ln \left(\frac{R}{Nh} \right) + \left(\frac{\Delta S_{\text{act}}}{R} \right) - \left(\frac{\Delta H_{\text{act}}}{RT} \right) \quad (5)$$

Hence, (h) is "planks constant"(6.626*10⁻³⁴ J.S), (N) is "Avogadro's number" (6.022*10²³ mol⁻¹), ($\ln \frac{i_{\text{corr}}}{T}$) vs. ($\frac{1}{T}$) can be drawn. Here, a straight line slope depicts its values ($-\frac{\Delta H_{\text{act}}}{R}$) and the intersections reveal it values ($\ln \frac{R}{Nh} + \frac{\Delta S_{\text{act}}}{R}$), as indicated in Figure 1 and Table 3.

The rise of the Arrhenius coefficient

becomes stable showing high reaction rates, yet activation energy reduction reveals the Arrhenius coefficient stability in a low reaction rates. The activating energy variations and the Arrhenius coefficient are clear in which reacting corrosion starts with sites showing low activating cards spreading to higher activation energy sites [21].

So, adding inhibitors raises the energy barriers of copper corrosions in the solutions with chlorine ions, while corrosions show and that the inhibitors postpone it. Also, temperature increase raises the corrosion and then decreased the inhibition efficiency in which rises in inhibitor concentration increases the densities of electrons in the adsorption centers of the molecules of the inhibitor improving the inhibition efficiency [22].

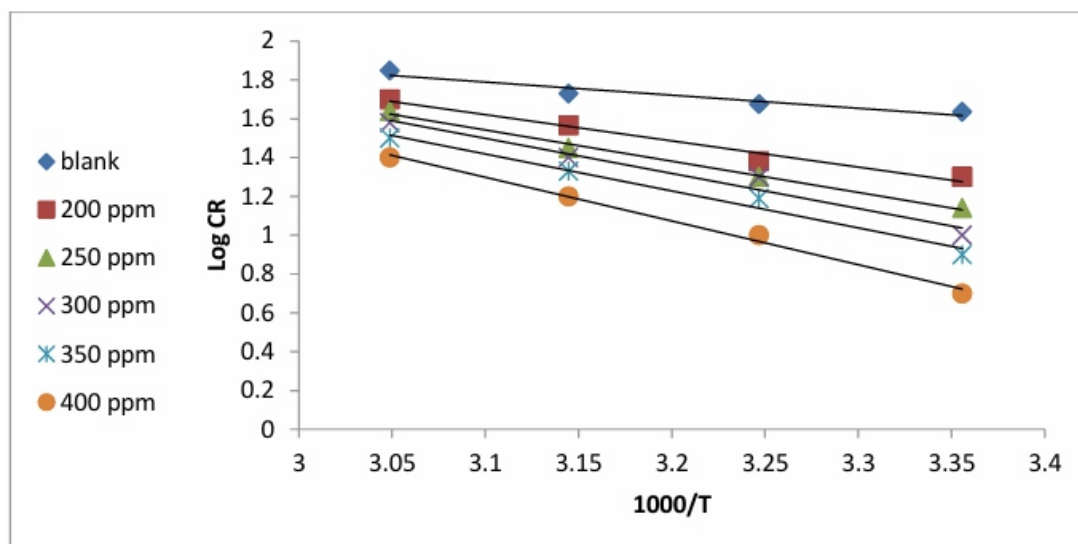


FIGURE 1 Log CR_r Arrhenius plots vs. 1/T for the corrosions of copper in 0.5 M HNO₃ with and without concentrations of garlic extract

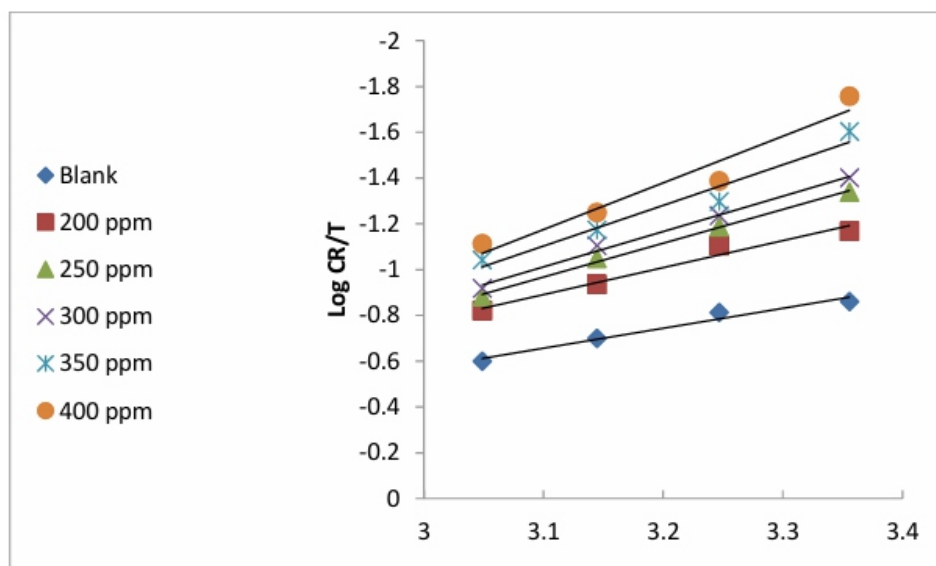


FIGURE 2 Arrhenius of log (CR/T) plots 1/T for the copper corrosions in 0.5 M HNO₃ with various concentrations of garlic extracts

TABLE 3 Activating energy's (E_a), activating enthalpies (ΔH_a), and the entropies of activations (ΔS_a) for the copper corrosions in 0.5 M with and with no inhibitor

Conc. (ppm)	E _a (KJ.mol ⁻¹)	ΔH _a (KJ. mol ⁻¹)	-ΔS _a (J.K ⁻¹ .mol ⁻¹)
Blank	13	16	158,9
200	26	22.6	144
250	30.6	28	128
300	34.5	30	125
350	36.4	34	113
400	44	39	99.6

The adsorption isotherm The surface coverage data is important in evaluating the inhibitor features and it is valuable in the discussion of the adsorption features with the isotherm adsorption help as adding inhibitor molecules on the surfaces in the metal interaction with them.

The examination of the outer coverage (θ), of the operating electrode (copper) surfaces through the inhibitors (garlic extract) and the concentrations of inhibitors' solutions (C_{inh}) are conducted fitting different adsorption isotherms. The best was gotten with Langmuir isotherm given by the next equation [23,24]

$$\frac{C_{inh}}{\theta} = \frac{1}{K_{adc}} + C_{inh} \quad (6)$$

Where, K_{ads} is the equilibrium constant of the adsorption/desorption reflecting that the inhibitor molecules are approaching the surface adsorption sites. The measured K_{ads} the Gibbs free energies of adsorption were measured by [25].

$$\Delta G^{\circ}_{ads} = -RT \ln (55.5 K_{ads}) \quad (7)$$

In which, R is gas constants, T is the absolute temperatures and the values (55.5) are the molar water concentrations in mol/L, while the standard enthalpies of adsorption are measured by the van't Hoff formula;

$$\ln K_{ads} = -\frac{\Delta H_{ads}}{RT} + \text{constant} \quad (8)$$

Plots of $\ln K_{ads}$ values vs. $1/T$ values showed the straight lines slope equal $\frac{-\Delta H_{ads}}{R}$. The negative ΔH° values revealed adsorption of garlic extract molecules as exothermic. The ΔG° negative values with the inhibitor are followed by exothermic adsorption processes. ΔS°_{ads} of inhibitions are measured from [26] as in Equation 4:

$$\Delta S^{\circ}_{ads} = \frac{\Delta H^{\circ}_{ads} - \Delta G^{\circ}_{ads}}{T} \quad (9)$$

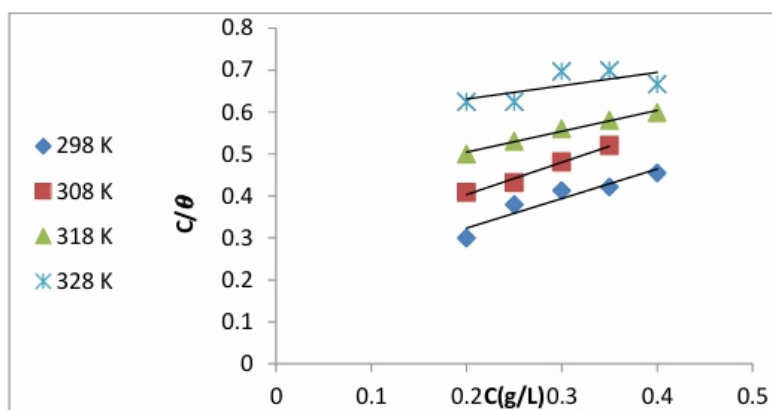


FIGURE 3 Langmuir isotherm plots to the (garlic extract) adsorptions on coppers in 0.5 HNO₃

TABLE 4 Thermodynamic parameters for the adsorptions of garlic extract on copper in 0.5 M HNO₃

T K	K _{ads} (g ⁻¹ .L)	-ΔG ^o _{ads} (kJ.mol ⁻¹)	-ΔH ^o _{ads} (kJ.mol ⁻¹)	ΔS ^o _{ads} (J.K ⁻¹ .mol ⁻¹)
298	5.5	14.174		
308	4.0	13.834		
318	2.5	13.041	30	53
328	1.8	12.555		

ΔG^o values reached -20kJ/mol were considered as the electrostatic of the charged molecules interacting with the metal outer layers (physisorption). Yet, the ΔG_{ads} values are more negative than -40kJ/mol as charges in common or transferring from the molecules of the inhibitors to the metal surfaces to form coordinating covalent bonds(chemisorption). The ΔG^o values ranged (12-14) kJ.mole⁻¹, meaning the inhibitor adsorption on copper alloy surfaces happen by physical adsorptions [27].

The negative values of ΔH^o indicate adsorption of the inhibitor molecules as exothermic. The adsorption could be either chemical or physical, yet the positive value shows an endothermic aspect attributed to chemisorption. Thus, the adsorption of the garlic extracts molecules on the surfaces refer for physisorption in this article [28].

Scanning electron microscope (SEM) measurements

Surface of copper were analyzed by SEM to verify the absorption of the extracted molecules as adsorbed on the surfaces of the copper alloys or just peeled off the surfaces. The SEM micrograph for copper alloy surfaces following their immersing in 0.5 M of nitric acid adding or not adding the ideal concentrations of garlic extract as in Figure 4 in which in Figure a is polished alloys of copper, (b) copper alloys immersed in nitric acids (HNO₃), and (c) copper alloys in (0.5) of M(HNO₃) solutions with a 400 ppm of garlic extracts comparing the SEM micrographs with and without the extract shows the great inhibitive effects of those compounds.

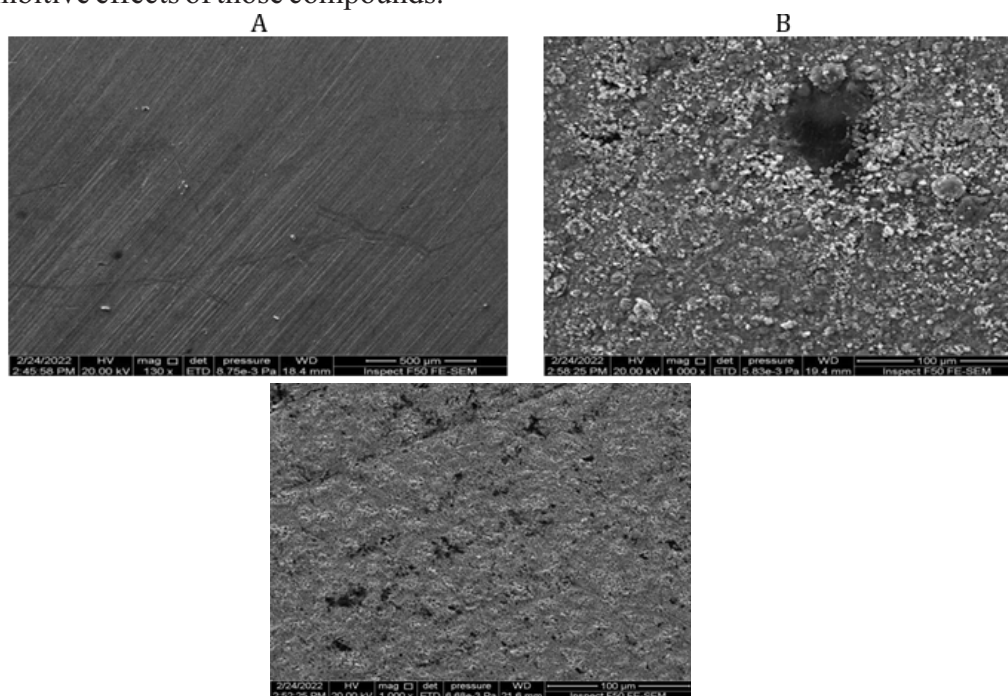


FIGURE 4 Scan of the micrographs of the electron(a) polished copper alloys, (b) copper alloys immersed in nitric acids (HNO₃), and (c) n copper alloys in (0.5)ofM(HNO₃) solutions with a 400 ppm of garlic extracts

Conclusion

The results of this study indicated that garlic extract an efficient inhibitor for copper in 1M (HNO₃) solutions by using weight loss techniques. The negative values of ΔG reveal that the adsorption of the inhibitors on the metal surface is spontaneous. Furthermore, E_a and ΔH values of the corrosion support this observation. All values of ΔS^*_{ads} are negative for the blank and inhibited solution which implies that the activation complex in the rate determining step represents association dissociation step. The rather than adsorption characteristics of garlic extract on the metal surface were approximated by Langmuir adsorption isotherm, and it obeyed and fitted this model. The protection efficiency was enhanced with the increase of inhibitor concentration. The highest value reached 87.9% at 400 ppm of garlic extract.

Acknowledgements

The authors extend their acknowledgment to the Deanship of College of Education for Pure Science Ibn-Al-Haithamat University of Baghdad for supporting this research.

Conflict of Interest

The authors declare that there is no conflict of interests regarding the publication of this manuscript.

Orcid:

Nawras Saad Mohamed Ramadan: <https://www.orcid.org/0000-0001-7780-4048> Zainab Wajdi Ahmed: <https://www.orcid.org/0000-0001-8267-6212>

References

- [1] I.M. Chung, R. Malathy, S.H. Kim, K. Kalaiselvi, M. Prabakaran, M. Gopiraman, J. Adhes. Sci. Technol., 2020, 34, 1483–1506. [Crossref], [Google Scholar], [Publisher]
- [2] A.-R.I. Mohammed, M.M. Solomon, K. Haruna, S.A. Umoren, T.A. Saleh, Environ. Sci. Res., 2020, 27, 34270–34288. [Crossref], [Google Scholar], [Publisher]
- [3] K.F. Khaled, Corrosion Science, 2010, 52, 3225–3234. [Crossref], [Google Scholar], [Publisher]
- [4] B. El Ibrahim, A. AitAddi, L. Guo, S. Kaya, Anti Corrosive Materials, 2022, 297–321. [Crossref], [Google Scholar], [Publisher]
- [5] A. Miralrio, A. Espinoza Vázquez, Processes, 2020, 8, 942. [Crossref], [Google Scholar], [Publisher]
- [6] N. Bhardwaj, P. Sharma, V. Kumar, Corros. Rev., 2021, 39, 27–41. [Crossref], [Google Scholar], [Publisher]
- [7] V. Pourzarghan, B. Fazeli-Nasab, Herit. Sci., 2021, 9, 1–14. [Crossref], [Google Scholar], [Publisher]
- [8] M. Faiz, A. Zahari, K. Awang, H. Hussin, RSC Adv., 2020, 10, 6547–6562. [Crossref], [Google Scholar], [Publisher]

Scholar], [Publisher]

- [9] M. Mohanraj, S. Aejitha, AIP Publishing LLC, 2020, 2270, 50004. [Crossref], [Google Scholar], [Publisher]
- [10] R.T. Loto, C.A. Loto, Cogent Eng., 2020, 7, 1798579. [Crossref], [Google Scholar], [Publisher]
- [11] A. Zaher, A. Chaouiki, R. Salghi, A. Boukhraz, B. Bourkhiss, M. Ouhssine, Int. J. Corros., 2020, 2020, Article ID 9764206. [Crossref], [Google Scholar], [Publisher]
- [12] O.O. Ogunleye, A.O. Arinkoola, O.A. Eletta, O.O. Agbede, Y.A. Osho, A.F. Morakinyo, J.O. Hamed, Heliyon, 2020, 6, e03205. [Crossref], [Google Scholar], [Publisher]
- [13] A.E. Ali, G.E. Badr, S.F.A. El-Aziz, Biointerface Res. Appl. Chem., 2021, 11, 1400714020. [Crossref], [Google Scholar], [Pdf]
- [14] S. Mo, H.Q. Luo, N.B. Li, J. Colloid Interf. Sci., 2017, 505, 929-939. [Crossref], [Google Scholar], [Publisher]
- [15] Y. Abayomi, S.S. Fagbuaro, S.O.K. Fajemilehin, Journal of Bioscience and Biotechnology Discovery, 2018, 3, 105-109. [Crossref], [Google Scholar], [PDF]
- [16] F. Wedian, M.A. Al-Qudad, Gh.M. AlMazideh, Int. J. Electrochem. Sci., 2017, 12, 4664-4676. [Crossref], [Google Scholar], [Publisher]
- [17] T.T. Bataineh, M.A. Al-Qudah, Nawafleh, N.A.F. Al-Rawashdeh, Inter. J. Electrochem. Sci., 2014, 9, 3543-5357. [PDF], [Google Scholar], [Publisher]
- [18] F. Wedian, M.A. Al-Qudahand, G.M. AlMazaideh, Int. J. Electrochem. Sci., 2017, 12, 4664-4676. [Crossref], [Google Scholar], [Publisher]
- [19] H. Wang, Y. Liu, J. Xie, J. Tang, M. Duan, Y. Wang, M. Chamas, Int. J. Electrochem. Sci., 2016, 11, 4943-4956. [Crossref], [Google Scholar], [Pdf]
- [20] Z.K. Kuraimid, H.M. Majeed, H.Q. Jebur, T.H. Ahmed, O.S. Jaber, Eurasian Chem. Commun., 2021, 3, 860-871. [Crossref], [Pdf], [Publisher]
- [21] M.T. Mohammed, W.N. Al-Sieadi, Al-Jailawi, Eurasian Chem. Commun., 2022, 4, 481-494. [Crossref], [Pdf], [Publisher]
- [22] Z.W. Ahmed, J.A. Naser, A. Farooq, J. Chem., 2020, 63, 3703-3711. [Crossref], [Google Scholar], [Publisher]
- [23] Z.W. Ahmed, E.H. Ali, I.M. Radhi, Inter. J. Pharma. Research, 2020, 1, 2078. [Crossref], [Google Scholar], [Publisher]
- [24] N.H. Ali, I.M.H. Almousawi, I.Y. Mohammed, Eurasian Chem. Commun., 2021, 921-928. [Crossref], [Pdf],
- [25] W.A. Isa, Z.W. Ahmed, Ibn Al-Haitham Jour. for Pure & Appl. Sci., 2016, 29, 73-16. [Google Scholar], [Publisher]
- [26] E.H. Ali, J.A. Naser, Z.W. Ahmed, T.A. Himdan, Journal of Renewable Materials, 2021, 9, 1927-1939. [Crossref], [Google Scholar], [Publisher]
- [27] T. Laabaissi, M. Bouassiria, H. Oudda, H. Zarrok, A. Zarrouk, A. Elmidaoui, L. Lakhrissi, B. Lakhrissi, E.M. Essassi, R. Tuir, J. Mater. Environ. Sci., 2016, 7, 1538-1548. [Google Scholar], [Publisher]
- [28] T. Sasikala, K. Parameswari, S. Chitra, A. Kiruthika, Measurement, 2017, 101, 175-182. [Crossref], [Google Scholar], [Publisher]
- [29] A.R. Salih, Z.A.K. AL-Messari, ECC. 2021, 3, 533-541. [Crossref], [Google Scholar], [Publisher]
- [30] B.H.R. Wolffenbuttel, H.J.C.M. Wouters, M.R. Heiner-Fokkema, M.M. van der Klauw, MCP: IQ&O, 2019, 3, 200-214. [Crossref], [Google Scholar], [Publisher]

Study of middle graph for certain classes of graph by applying degree-based topological indices

Muhammad Shoaib Sardara,* |Muhammad Asad Alia |Faraha Ashrafa |Murat Cancanb

aSchool of Mathematics, Minhaj University, Lahore, Pakistan

bFaculty of Education, Van Yuzuncu Yıl University, Zeve Campus, Tuşba, 65080, Van, Turkey

ABSTRACT

Topological indices are extremely useful for analyzing various physical and chemical properties associated with a chemical compound. A topological index describes molecular structures by converting them into certain real numbers. Topological indices are used in the development of quantitative structure-activity relationships (QSARS) in which the biological activity of molecule correlated with their chemical structure. The chemical shape of benzene molecule is very common in nano-science, chemistry, and physics. The circumcoronene collection of benzenoid (HS) generates from the benzene molecules. Jahangir graph is a generalized wheel graph that consists of (m,t) circular vertices and a center vertex connected to every mt vertex on the circle. In this article, we will compute the topological indices of the middle graph of the circumcoronene series of benzenoids (hs) and Jahangir graph. In addition, comparison of the middle graph of the circumcoronene series of benzenoid (HS) and Jahangir graph are presented numerically and graphically

KEYWORDS Topological Indices; circumcoronene series of benzenoid; middle graph; Jahangir graph.

INTRODUCTION

Consider a molecular graph $G = (V, E)$, such a graph with vertex set $V(G)$ indicates the atoms and edge set $E(G)$ indicates chemical bonds. A degree is represented by d_θ $\{\theta \in V(G)\}$ which is defined as the number of edges incident with (θ) . (For unspecified terminologies and more details [1]). Graph theory is branch of mathematics that has been applied in virtually every field of study. The usage of topological indices in QSPR/ QSAR studies has taken important concentration in recent years. Graph theory is used to assess the linkage among several topological indices of certain graphs that generated by some graph operations that are middle graph, total graph, semi-total graph, and the strong double graph etc. Topological indices are numerical parameters of a graph studies has taken important concentration in recent years. Graph theory is used to assess the linkage among several topological indices of certain graphs that generated by some graph operations that are middle graph, total graph, semi-total graph, and the strong double graph etc. Topological indices are numerical parameters of a graph.

The symmetric division degree index (SD) of connected graph (G) [4] is defined as Follows:

$$SD(G) = \sum_{\theta\omega \in E(G)} \frac{d_\theta^2 + d_\omega^2}{d_\theta d_\omega} \quad (1)$$

where, d_{θ} and d_w are the degrees of vertex θ , and w in G .

The sum-Connectivity index [5] is defined as follows:

$$SC(G) = \sum_{\theta w \in E(G)} \frac{1}{\sqrt{d_{\theta} + d_w}}. \quad (2)$$

Randic connectivity index is widely used in mathematical chemistry, due to its wide applications in both mathematics and chemistry. It is defined [6] in the following equation:

$$RC(G) = \sum_{\theta w \in E(G)} \frac{1}{\sqrt{d_{\theta} d_w}}. \quad (3)$$

The First-Zagreb index [7] is defined as:

$$M_1(G) = \sum_{\theta w \in E(G)} (d_{\theta} + d_w) \quad (4)$$

The second-Zagreb index [7] is defined as:

$$M_2(G) = \sum_{\theta w \in E(G)} (d_{\theta} d_w). \quad (5)$$

Zhong introduced the harmonic index in 2012 which is defined [8] as follows:

$$H(G) = \sum_{\theta w \in E(G)} \frac{2}{(d_{\theta} + d_w)}. \quad (6)$$

For more wide-ranging and comprehensive details, we offer the readers to follow the following articles [9-13, 17-40].

Definition 1.1. A graph that contains a cycle C_{mt} having an extra vertex which is adjacent to t vertices of C_{mt} at the distance m to each other on the C_{mt} . In Jahngir graph [14] ($J_{m,t}$), where $t \geq 2$ and $m \geq 3$. The number of vertices and edges is $mt + 1$ and $mt + m$ respectively. Jahangir graphs $J_{(3,2)}$ and $J_{(3,3)}$ are displayed in Figure 1

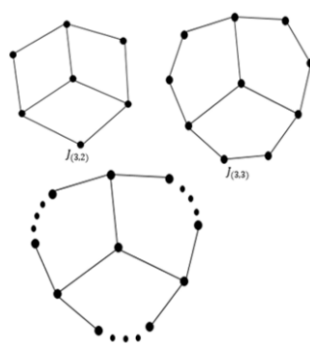


FIGURE 1 Jahangir graph

Definition 1.2. Circumcoronene series of benzenoid (H_s) where, ($s \geq 1$) is one family that is generated from benzene c 6 on circumference [15]. The number of vertices are $6s^2$ and edges are $9s^2 - 3s$, in this of benzenoid. The Circumcoronene series of benzenoids are designated in Figure 2.

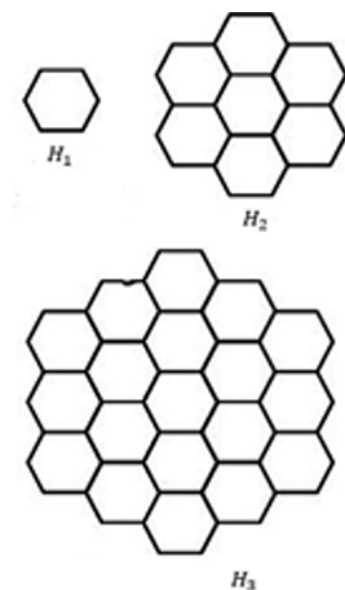


FIGURE 2 Circumcoronene series of benzenoid

Definition 1.3. The middle graph [16] of any graph G is attained by adding a new vertex to each of its edge and connecting by edges any pairs of those new vertices which lie on the adjacent edges of the graph. The middle graph of graph G is represented by $M(G)$. For example, the middle graph of the Jahangir graph ($J_{(3,3)}$) is depicted in Figure 3.

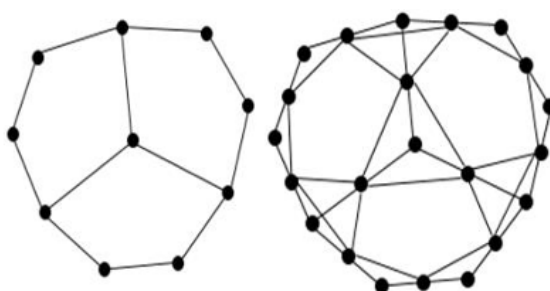


FIGURE 3 Jahangir Graph ($J_{(3,3)}$) and its middle graph [$M(J_{(3,3)})$]

Result for the Middle Graph of Jahangir graph $J_{(3,t)}$

In this section, we calculate degree-based indices of the middle graph of Jahangir graph $J_{(3,t)}$, where $t \geq 3$.

Theorem 2.1. Let $[M(J_{(3,t)})]$ be the middle graph of Jahangir graph. Then,

$$\begin{aligned} 1. SD[M(J_{(3,t)})] &= \frac{3(14t+23)}{2}. \\ 2. SC[M(J_{(3,t)})] &= \sqrt{6}t + \frac{3t}{\sqrt{8}} - 2\sqrt{6} - \frac{9}{\sqrt{8}} + 4 \\ &+ \frac{6}{\sqrt{7}} + \frac{3}{\sqrt{2}} + \frac{3}{\sqrt{10}} + \frac{6}{\sqrt{11}} + \frac{\sqrt{3}}{2}. \\ 3. RC[M(J_{(3,t)})] &= \frac{((4\sqrt{3}+12)\sqrt{5}+30t-40)\sqrt{2}}{20} \\ &+ \frac{(8\sqrt{3}+12)\sqrt{5}+15t-23}{20}. \end{aligned}$$

$$4. H[M(J_{(3,t)})] = \frac{11t}{4} + \frac{8417}{4620}.$$

$$5. M_1[M(J_{(3,t)})] = 60t + 186.$$

$$6. M_2[M(J_{(3,t)})] = 96t + 501.$$

Proof: The middle graph of Jahangir graph $M(J_{(3,t)})$ has 4 vertices of degree 3 and 6 vertices of degree 5, $3(t-2)$ vertices of degree 4, $3t-3$ vertices of degree 2 and 3 vertices of degree 6.

In $M(J_{(3,t)})$, we get edges of type $E_{(2,4)}$, $E_{(2,5)}$, $E_{(3,5)}$, $E_{(3,6)}$, $E_{(4,4)}$, $E_{(4,5)}$, $E_{(5,5)}$, $E_{(5,6)}$, and $E_{(6,6)}$. The number of edges of these types are given in Table 1.

TABLE 1 Edge division

$E[d_u, d_v]$	$E_{(2,4)}$	$E_{(2,5)}$	$E_{(3,5)}$	$E_{(3,6)}$	$E_{(4,4)}$	$E_{(4,5)}$	$E_{(5,5)}$	$E_{(5,6)}$	$E_{(6,6)}$
Number of edges	$6t-12$	6	6	6	$3t-9$	6	3	6	3

By using Table 1 and the Equation (1), we get the desired results, i.e.,

$$\begin{aligned} SD[M(J_{(3,t)})] &= \sum_{\theta\omega \in E(M(J_{(3,t)}))} \frac{d_\theta^2 + d_\omega^2}{d_\theta d_\omega} \\ SD[M(J_{(3,t)})] &= E_{(2,4)} \sum_{\theta\omega \in E(M(J_{(3,t)}))} \frac{d_\theta^2 + d_\omega^2}{d_\theta d_\omega} \\ &+ E_{(2,5)} \sum_{\theta\omega \in E(M(J_{(3,t)}))} \frac{d_\theta^2 + d_\omega^2}{d_\theta d_\omega} \\ &+ E_{(3,5)} \sum_{\theta\omega \in E(M(J_{(3,t)}))} \frac{d_\theta^2 + d_\omega^2}{d_\theta d_\omega} \\ &+ E_{(3,6)} \sum_{\theta\omega \in E(M(J_{(3,t)}))} \frac{d_\theta^2 + d_\omega^2}{d_\theta d_\omega} \\ &+ E_{(4,4)} \sum_{\theta\omega \in E(M(J_{(3,t)}))} \frac{d_\theta^2 + d_\omega^2}{d_\theta d_\omega} \\ &+ E_{(4,5)} \sum_{\theta\omega \in E(M(J_{(3,t)}))} \frac{d_\theta^2 + d_\omega^2}{d_\theta d_\omega} \end{aligned}$$

$$\begin{aligned} &+ E_{(5,5)} \sum_{\theta\omega \in E(M(J_{(3,t)}))} \frac{d_\theta^2 + d_\omega^2}{d_\theta d_\omega} \\ &+ E_{(5,6)} \sum_{\theta\omega \in E(M(J_{(3,t)}))} \frac{d_\theta^2 + d_\omega^2}{d_\theta d_\omega} \\ &+ E_{(6,6)} \sum_{\theta\omega \in E(M(J_{(3,t)}))} \frac{d_\theta^2 + d_\omega^2}{d_\theta d_\omega}. \\ SD[M(J_{(3,t)})] &= (6t-12) \frac{(2)^2 + (4)^2}{8} \\ &+ (6) \frac{(2)^2 + (5)^2}{10} \\ &+ (6) \frac{(3)^2 + (5)^2}{15} \\ &+ (6) \frac{(3)^2 + (6)^2}{18} \\ &+ (3t-9) \frac{(4)^2 + (4)^2}{16} \\ &+ (6) \frac{(4)^2 + (5)^2}{20} \\ &+ (3) \frac{(5)^2 + (5)^2}{25} \\ &+ (6) \frac{(5)^2 + (6)^2}{30} \\ &+ (3) \frac{(6)^2 + (6)^2}{36} \end{aligned}$$

$$[M(J_{(3,t)})] = (3t - 6)5 + \frac{216}{5} + (3t - 9)2 + 27 + \frac{123}{10}$$

$$SD[M(J_{(3,t)})] = 21t + 29.5.$$

$$SC(G) = \sum_{\theta\omega \in E(G)} \frac{1}{\sqrt{d_\theta + d_\omega}}$$

$$SC[M(J_{(3,t)})]$$

$$= E_{(2,4)} \sum_{\theta\omega \in E(M(J_{(3,t)}))} \frac{1}{\sqrt{d_\theta + d_\omega}}$$

$$+ E_{(2,5)} \sum_{\theta\omega \in E(M(J_{(3,t)}))} \frac{1}{\sqrt{d_\theta + d_\omega}}$$

$$+ E_{(3,5)} \sum_{\theta\omega \in E(M(J_{(3,t)}))} \frac{1}{\sqrt{d_\theta + d_\omega}}$$

$$+ E_{(3,6)} \sum_{\theta\omega \in E(M(J_{(3,t)}))} \frac{1}{\sqrt{d_\theta + d_\omega}}$$

$$+ E_{(4,4)} \sum_{\theta\omega \in E(M(J_{(3,t)}))} \frac{1}{\sqrt{d_\theta + d_\omega}}$$

$$+ E_{(4,5)} \sum_{\theta\omega \in E(M(J_{(3,t)}))} \frac{1}{\sqrt{d_\theta + d_\omega}}$$

$$+ E_{(5,5)} \sum_{\theta\omega \in E(M(J_{(3,t)}))} \frac{1}{\sqrt{d_\theta + d_\omega}}$$

$$+ E_{(5,6)} \sum_{\theta\omega \in E(M(J_{(3,t)}))} \frac{1}{\sqrt{d_\theta + d_\omega}}$$

$$+ E_{(6,6)} \sum_{\theta\omega \in E(M(J_{(3,t)}))} \frac{1}{\sqrt{d_\theta + d_\omega}}$$

$$SC[M(J_{(3,t)})] = (6t - 12) \frac{1}{\sqrt{6}} + (6) \frac{1}{\sqrt{7}}$$

$$+ (6) \frac{1}{\sqrt{8}} + (6) \frac{1}{\sqrt{9}}$$

$$+ (3t - 9) \frac{1}{\sqrt{8}} + (6) \frac{1}{\sqrt{9}}$$

$$+ (3) \frac{1}{\sqrt{10}} + (6) \frac{1}{\sqrt{11}}$$

$$+ (3) \frac{1}{\sqrt{12}}$$

$$SC[M(J_{(3,t)})] = \sqrt{6}t + \frac{3t}{\sqrt{8}} - 2\sqrt{6} - \frac{9}{\sqrt{8}} + 4 + \frac{6}{\sqrt{7}} + \frac{3}{\sqrt{2}} + \frac{3}{\sqrt{10}} + \frac{6}{\sqrt{11}} + \frac{\sqrt{3}}{2}.$$

$$RC(G) = \sum_{\theta\omega \in E(G)} \frac{1}{\sqrt{d_\theta d_\omega}}$$

$$RC[M(J_{(3,t)})] = E_{(2,4)} \sum_{\theta\omega \in E(M(J_{(3,t)}))} \frac{1}{\sqrt{d_\theta d_\omega}}$$

$$+ E_{(2,5)} \sum_{\theta\omega \in E(M(J_{(3,t)}))} \frac{1}{\sqrt{d_\theta d_\omega}}$$

$$+ E_{(3,5)} \sum_{\theta\omega \in E(M(J_{(3,t)}))} \frac{1}{\sqrt{d_\theta d_\omega}}$$

$$+ E_{(3,6)} \sum_{\theta\omega \in E(M(J_{(3,t)}))} \frac{1}{\sqrt{d_\theta d_\omega}}$$

$$+ E_{(4,4)} \sum_{\theta\omega \in E(M(J_{(3,t)}))} \frac{1}{\sqrt{d_\theta d_\omega}}$$

$$+ E_{(4,5)} \sum_{\theta\omega \in E(M(J_{(3,t)}))} \frac{1}{\sqrt{d_\theta d_\omega}}$$

$$+ E_{(5,5)} \sum_{\theta\omega \in E(M(J_{(3,t)}))} \frac{1}{\sqrt{d_\theta d_\omega}}$$

$$+ E_{(5,6)} \sum_{\theta\omega \in E(M(J_{(3,t)}))} \frac{1}{\sqrt{d_\theta d_\omega}}$$

$$+ E_{(6,6)} \sum_{\theta\omega \in E(M(J_{(3,t)}))} \frac{1}{\sqrt{d_\theta d_\omega}}.$$

$$RC[M(J_{(3,t)})] = (6t - 12) \frac{1}{\sqrt{8}} + (6) \frac{1}{\sqrt{10}}$$

$$+ (6) \frac{1}{\sqrt{15}} + (6) \frac{1}{\sqrt{18}}$$

$$+ (3t - 9) \frac{1}{\sqrt{16}} + (6) \frac{1}{\sqrt{20}}$$

$$+ (3) \frac{1}{\sqrt{25}} + (6) \frac{1}{\sqrt{30}}$$

$$+ (3) \frac{1}{\sqrt{36}}$$

$$RC[M(J_{(3,t)})] = \left(\frac{3}{4} + \frac{3}{\sqrt{2}}\right)t + \frac{3}{\sqrt{5}} - 2\sqrt{2} + \sqrt{\frac{6}{5}} \\ + 2\sqrt{\frac{3}{5}} + 3\sqrt{\frac{2}{5}} - \frac{23}{20}.$$

$$H(G) = \sum_{\theta\omega \in E(G)} \frac{2}{(d_\theta + d_\omega)} \\ H[M(J_{(3,t)})] \\ = E_{(2,4)} \sum_{\theta\omega \in E(M(J_{(3,t)}))} \frac{2}{(d_\theta + d_\omega)} \\ + E_{(2,5)} \sum_{\theta\omega \in E(M(J_{(3,t)}))} \frac{2}{(d_\theta + d_\omega)} \\ + E_{(3,5)} \sum_{\theta\omega \in E(M(J_{(3,t)}))} \frac{2}{(d_\theta + d_\omega)} \\ + E_{(3,6)} \sum_{\theta\omega \in E(M(J_{(3,t)}))} \frac{2}{(d_\theta + d_\omega)} \\ + E_{(4,4)} \sum_{\theta\omega \in E(M(J_{(3,t)}))} \frac{2}{(d_\theta + d_\omega)} \\ + E_{(4,5)} \sum_{\theta\omega \in E(M(J_{(3,t)}))} \frac{2}{(d_\theta + d_\omega)} \\ + E_{(5,5)} \sum_{\theta\omega \in E(M(J_{(3,t)}))} \frac{2}{(d_\theta + d_\omega)} \\ + E_{(5,6)} \sum_{\theta\omega \in E(M(J_{(3,t)}))} \frac{2}{(d_\theta + d_\omega)} \\ + E_{(6,6)} \sum_{\theta\omega \in E(M(J_{(3,t)}))} \frac{2}{(d_\theta + d_\omega)} \\ H[M(J_{(3,t)})] = (6t - 12)\frac{2}{6} + (6)\frac{2}{7} + (6)\frac{2}{8} \\ + (6)\frac{2}{9} + (3t - 9)\frac{2}{8} + (6)\frac{2}{9} \\ + (3)\frac{2}{10} + (6)\frac{2}{11} + (3)\frac{2}{12}. \\ H[M(J_{(3,t)})] = (2t - 4) + \frac{12}{7} + \frac{3}{2} + \frac{4}{3} \\ + (3t - 9)\frac{1}{4} + \frac{4}{3} + \frac{3}{5} + \frac{12}{11} + \frac{1}{2} \\ H[M(J_{(3,t)})] = \frac{11t}{4} + \frac{8417}{4620}.$$

$$M_1(G) = \sum_{\theta\omega \in E(G)} (d_\theta + d_\omega). \\ M_1[M(J_{(3,t)})] = E_{(2,4)} \sum_{\theta\omega \in E(M(J_{(3,t)}))} (d_\theta + d_\omega) \\ + E_{(2,5)} \sum_{\theta\omega \in E(M(J_{(3,t)}))} (d_\theta + d_\omega) \\ + E_{(3,5)} \sum_{\theta\omega \in E(M(J_{(3,t)}))} (d_\theta + d_\omega) \\ + E_{(3,6)} \sum_{\theta\omega \in E(M(J_{(3,t)}))} (d_\theta + d_\omega) \\ + E_{(4,4)} \sum_{\theta\omega \in E(M(J_{(3,t)}))} (d_\theta + d_\omega) \\ + E_{(4,5)} \sum_{\theta\omega \in E(M(J_{(3,t)}))} (d_\theta + d_\omega) \\ + E_{(5,5)} \sum_{\theta\omega \in E(M(J_{(3,t)}))} (d_\theta + d_\omega) \\ + E_{(5,6)} \sum_{\theta\omega \in E(M(J_{(3,t)}))} (d_\theta + d_\omega) \\ + E_{(6,6)} \sum_{\theta\omega \in E(M(J_{(3,t)}))} (d_\theta + d_\omega). \\ M_1[M(J_{(3,t)})] = (6t - 12)6 + (6)7 + (6)8 \\ + (6)9 + (3t - 9)8 + (6)9 \\ + (3)10 + (6)11 + (3)12. \\ M_1[M(J_{(3,t)})] = 36t - 72 + 42 + 48 + 54 \\ + 24t - 72 + 54 + 30 + 66 \\ + 36. \\ M_1[M(J_{(3,t)})] = 60t + 186. \\ M_2(G) = \sum_{\theta\omega \in E(G)} (d_\theta d_\omega)$$

$$\begin{aligned}
M_2[M(J_{(3,t)})] &= E_{(2,4)} \sum_{\theta\omega \in E(M(J_{(3,t)}))} (d_\theta d_\omega) + E_{(2,5)} \sum_{\theta\omega \in E(M(J_{(3,t)}))} (d_\theta d_\omega) \\
&+ E_{(3,5)} \sum_{\theta\omega \in E(M(J_{(3,t)}))} (d_\theta d_\omega) + E_{(3,6)} \sum_{\theta\omega \in E(M(J_{(3,t)}))} (d_\theta d_\omega) \\
&+ E_{(4,4)} \sum_{\theta\omega \in E(M(J_{(3,t)}))} (d_\theta d_\omega) + E_{(4,5)} \sum_{\theta\omega \in E(M(J_{(3,t)}))} (d_\theta d_\omega) \\
&+ E_{(5,5)} \sum_{\theta\omega \in E(M(J_{(3,t)}))} (d_\theta d_\omega) + E_{(5,6)} \sum_{\theta\omega \in E(M(J_{(3,t)}))} (d_\theta d_\omega) \\
&+ E_{(6,6)} \sum_{\theta\omega \in E(M(J_{(3,t)}))} (d_\theta d_\omega). \\
M_2[M(J_{(3,t)})] &= (6t - 12)8 + (6)10 + (6)15 \\
&+ (6)18 + (3t - 9)16 + (6)20 \\
&+ (3)25 + (6)30 + (3)36. \\
M_2[M(J_{(3,t)})] &= 48t - 96 + 60 + 90 + 108 \\
&+ 48n - 144 + 120 + 75 \\
&+ 180 + 108. \\
M_2[M(J_{(3,t)})] &= 96t + 501.
\end{aligned}$$

Comparison

In this section, we give comparison of the above-computed topological indices numerically and the graphically. The numerical comparison of the middle graph of Jahangir graph $J_{(3,t)}$ is demonstrated in Table 2, where $t = 2, 3, \dots, 10$ and graphically comparison is depicted in the Figure 4.

TABLE 2 Numerical result of middle graph of Jahangir graph $J_{(3,t)}$

t	$SD[M(J_{(3,t)})]$	$SC[M(J_{(3,t)})]$	$RC[M(J_{(3,t)})]$	$H[M(J_{(3,t)})]$	$M_1[M(J_{(3,t)})]$	$M_2[M(J_{(3,t)})]$
2	76.5	10.0476	7.6478	7.3218	306	693
3	97.5	13.5578	10.5191	10.0718	366	789
4	118.5	17.0679	13.3905	12.8218	426	885
5	139.5	20.5781	16.2618	15.5718	486	981
6	160.5	24.0882	19.1331	18.3218	546	1077
7	181.5	27.5984	22.0044	21.0718	606	1173
8	202.5	31.1085	24.8757	23.8218	666	1269
9	223.5	34.6187	27.7471	26.5718	726	1365
10	244.5	38.1288	30.6184	29.3218	786	1461

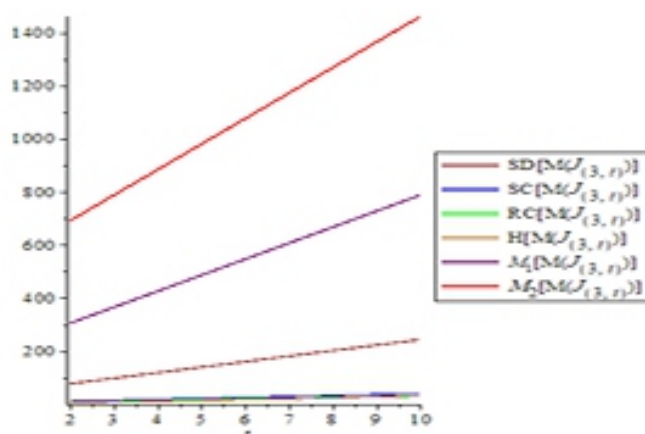


FIGURE 4 Graphical representation of middle graph of Jahangir graph $J_{(3,t)}$

Result for the Middle Graph of Circumcoronene Series of Benzenoid Graph (H_s)

In this section, we calculate the degree-based indices of the middle graph of (H_s), where $s \geq 2$.

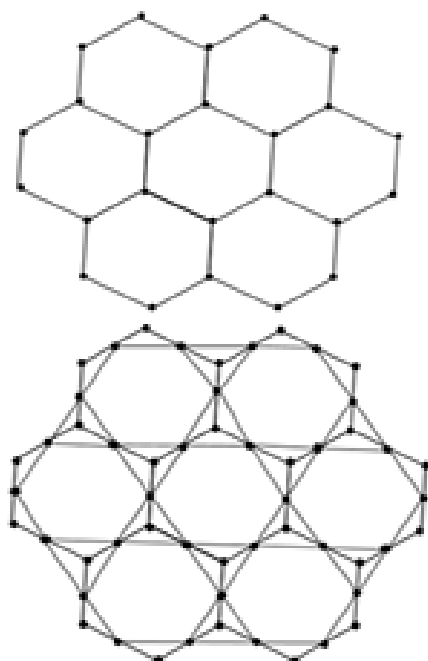


FIGURE 5 Circumcoronene series of benzenoid (H_2) and its middle graph $M(H_2)$

Theorem 4.1. Let $[M(H_s)]$ be the middle graph of circumcoronene series of benzenoid. Then,

$$\begin{aligned}
 SD[M(H_s)] &= \frac{273}{5} \\
 &+ (s-1) \left(\frac{174}{5} + \frac{136}{5} + \frac{122}{5} \right) \\
 &+ (18s^2 - 30s + 12) \frac{5}{2} - 48s \\
 &+ 36s^2. \\
 SC[M(H_s)] &= \frac{12}{\sqrt{6}} + (s-1) \left(\frac{12}{\sqrt{7}} + \frac{6}{\sqrt{2}} + \frac{12}{\sqrt{11}} \right) \\
 &+ 6s^2 - 10s + 8 + \frac{6(2s-3)}{\sqrt{10}} \\
 &+ \frac{9(s^2 - 2s + 1)}{\sqrt{3}}.
 \end{aligned}$$

$$\begin{aligned}
 RC[M(H_s)] &= \frac{6}{\sqrt{2}} \\
 &+ (s-1) \left(\frac{12}{\sqrt{10}} + \frac{12}{\sqrt{15}} + \frac{12}{\sqrt{30}} \right) \\
 &+ (6s^2 - 10s + 4) \frac{1}{\sqrt{2}} + \frac{6}{\sqrt{5}} \\
 &+ (2s-3) \frac{6}{5} + 3s^2 - 6s + 3. \\
 H[M(H_s)] &= \frac{1913}{1155}s + \frac{142}{1155} + 7s^2. \\
 M_1[M(H_s)] &= 378s^2 - 270s + 12. \\
 M_2[M(H_s)] &= 972s^2 - 876s + 90.
 \end{aligned}$$

Proof: The middle graph of circumcoronene series of benzenoid $M(H_s)$ where, $s \geq 2$ has: $6s$ vertices of degree 2, $6s(s-1)$ vertices of degree 3, 6 vertices of degree 4, $6s$ vertices of degree 5 and $9s^2 - 9s - 6$ vertices of degree 6.

In $M(H_s)$, we get edge of type $E_{(2,4)}$, $E_{(2,5)}$, $E_{(3,5)}$, $E_{(3,6)}$, $E_{(4,5)}$, $E_{(5,5)}$, $E_{(5,6)}$, and $E_{(6,6)}$. Table 3 lists the number of edges.

Now by using Table 3 and the Equation (1) we obtain the desired results, i.e.,

TABLE 3 Edge division

$E[d_u, d_v]$	Number of edges
$E_{(2,4)}$	12
$E_{(2,5)}$	$12(s-1)$
$E_{(3,5)}$	$12(s-1)$
$E_{(3,6)}$	$18s^2 - 30s + 12$
$E_{(4,5)}$	12
$E_{(5,5)}$	$6(2s-3)$
$E_{(5,6)}$	$12(s-1)$
$E_{(6,6)}$	$18(s^2 - 2s + 1)$

$$SD[M(J_{(3,t)})] = \sum_{\theta\omega \in E(G)} \frac{d_\theta^2 + d_\omega^2}{d_\theta d_\omega},$$

$$\begin{aligned}
SD[M(H_s)] &= E_{(2,4)} \sum_{\theta\omega \in E(M(H_s))} \frac{d_\theta^2 + d_\omega^2}{d_\theta d_\omega} \\
&+ E_{(2,5)} \sum_{\theta\omega \in E(M(H_s))} \frac{d_\theta^2 + d_\omega^2}{d_\theta d_\omega} \\
&+ E_{(3,5)} \sum_{\theta\omega \in E(M(H_s))} \frac{d_\theta^2 + d_\omega^2}{d_\theta d_\omega} \\
&+ E_{(3,6)} \sum_{\theta\omega \in E(M(H_s))} \frac{d_\theta^2 + d_\omega^2}{d_\theta d_\omega} \\
&+ E_{(4,5)} \sum_{\theta\omega \in E(M(H_s))} \frac{d_\theta^2 + d_\omega^2}{d_\theta d_\omega} \\
&+ E_{(5,5)} \sum_{\theta\omega \in E(M(H_s))} \frac{d_\theta^2 + d_\omega^2}{d_\theta d_\omega} \\
&+ E_{(5,6)} \sum_{\theta\omega \in E(M(H_s))} \frac{d_\theta^2 + d_\omega^2}{d_\theta d_\omega} \\
&+ E_{(6,6)} \sum_{\theta\omega \in E(M(H_s))} \frac{d_\theta^2 + d_\omega^2}{d_\theta d_\omega}.
\end{aligned}$$

$$\begin{aligned}
SD[M(H_s)] &= (12) \frac{(2)^2 + (4)^2}{8} + 12(s \\
&- 1) \frac{(2)^2 + (5)^2}{10} + 12(s \\
&- 1) \frac{(3)^2 + (5)^2}{15} + (18s^2 \\
&- 30s + 12) \frac{(3)^2 + (6)^2}{18} \\
&+ (12) \frac{(4)^2 + (5)^2}{20} \\
&+ 6(2s - 3) \frac{(5)^2 + (5)^2}{25} + 12(s \\
&- 1) \frac{(5)^2 + (6)^2}{30} + 18(s^2 \\
&- 2s + 1) \frac{(6)^2 + (6)^2}{36}.
\end{aligned}$$

$$SD[M(H_s)] = 81s^2 - \frac{183s}{5} - \frac{9}{5}.$$

$$SC(G) = \sum_{\theta\omega \in E(G)} \frac{1}{\sqrt{d_\theta + d_\omega}}$$

$$\begin{aligned}
SC[M(H_s)] &= E_{(2,4)} \sum_{\theta\omega \in E(M(H_s))} \frac{1}{\sqrt{d_\theta + d_\omega}} \\
&+ E_{(2,5)} \sum_{\theta\omega \in E(M(H_s))} \frac{1}{\sqrt{d_\theta + d_\omega}} \\
&+ E_{(3,5)} \sum_{\theta\omega \in E(M(H_s))} \frac{1}{\sqrt{d_\theta + d_\omega}} \\
&+ E_{(3,6)} \sum_{\theta\omega \in E(M(H_s))} \frac{1}{\sqrt{d_\theta + d_\omega}} \\
&+ E_{(4,5)} \sum_{\theta\omega \in E(M(H_s))} \frac{1}{\sqrt{d_\theta + d_\omega}} \\
&+ E_{(5,5)} \sum_{\theta\omega \in E(M(H_s))} \frac{1}{\sqrt{d_\theta + d_\omega}} \\
&+ E_{(5,6)} \sum_{\theta\omega \in E(M(H_s))} \frac{1}{\sqrt{d_\theta + d_\omega}} \\
&+ E_{(6,6)} \sum_{\theta\omega \in E(M(H_s))} \frac{1}{\sqrt{d_\theta + d_\omega}}.
\end{aligned}$$

$$\begin{aligned}
SC[M(H_s)] &= (12) \frac{1}{\sqrt{6}} + 12(s-1) \frac{1}{\sqrt{7}} + 12(s \\
&- 1) \frac{1}{\sqrt{8}} + (18s^2 - 30s \\
&+ 12) \frac{1}{\sqrt{9}} + \frac{12}{\sqrt{9}} + 6(2s \\
&- 3) \frac{1}{\sqrt{10}} + 12(s-1) \frac{1}{\sqrt{11}} \\
&+ 18(s^2 - 2s + 1) \frac{1}{\sqrt{12}}
\end{aligned}$$

$$\begin{aligned}
SC[M(H_s)] &= \frac{12}{\sqrt{6}} + (s-1) \left(\frac{12}{\sqrt{7}} + \frac{6}{\sqrt{2}} + \frac{12}{\sqrt{11}} \right) \\
&+ 6s^2 - 10s + 8 + \frac{6(2s-3)}{\sqrt{10}} \\
&+ \frac{9(s^2 - 2s + 1)}{\sqrt{3}}.
\end{aligned}$$

$$RC(G) = \sum_{\theta\omega \in E(G)} \frac{1}{\sqrt{d_\theta d_\omega}}$$

$$\begin{aligned}
RC[M(H_s)] &= E_{(2,4)} \sum_{\theta\omega \in E(M(H_s))} \frac{1}{\sqrt{d_\theta d_\omega}} \\
&+ E_{(2,5)} \sum_{\theta\omega \in E(M(H_s))} \frac{1}{\sqrt{d_\theta d_\omega}} \\
&+ E_{(3,5)} \sum_{\theta\omega \in E(M(H_s))} \frac{1}{\sqrt{d_\theta d_\omega}} \\
&+ E_{(3,6)} \sum_{\theta\omega \in E(M(H_s))} \frac{1}{\sqrt{d_\theta d_\omega}} \\
&+ E_{(4,5)} \sum_{\theta\omega \in E(M(H_s))} \frac{1}{\sqrt{d_\theta d_\omega}} \\
&+ E_{(5,5)} \sum_{\theta\omega \in E(M(H_s))} \frac{1}{\sqrt{d_\theta d_\omega}} \\
&+ E_{(5,6)} \sum_{\theta\omega \in E(M(H_s))} \frac{1}{\sqrt{d_\theta d_\omega}} \\
&+ E_{(6,6)} \sum_{\theta\omega \in E(M(H_s))} \frac{1}{\sqrt{d_\theta d_\omega}}
\end{aligned}$$

$$\begin{aligned}
RC[M(H_s)] &= \frac{12}{\sqrt{8}} + 12(s-1)\frac{1}{\sqrt{10}} + 12(s-1)\frac{1}{\sqrt{15}} + (18s^2 - 30s \\
&+ 12)\frac{1}{\sqrt{18}} + \frac{12}{\sqrt{20}} + 6(2s-3)\frac{1}{\sqrt{25}} + 12(s-1)\frac{1}{\sqrt{30}} \\
&+ 18(s^2 - 2s + 1)\frac{1}{\sqrt{36}}
\end{aligned}$$

$$\begin{aligned}
RC[M(H_s)] &= \frac{6}{\sqrt{2}} \\
&+ (s-1)\left(\frac{12}{\sqrt{10}} + \frac{12}{\sqrt{15}} + \frac{12}{\sqrt{30}}\right) \\
&+ (6s^2 - 10s + 4)\frac{1}{\sqrt{2}} + \frac{6}{\sqrt{5}} \\
&+ (2s-3)\frac{6}{5} + 3s^2 - 6s + 3.
\end{aligned}$$

$$H(G) = \sum_{\theta\omega \in E(G)} \frac{2}{(d_\theta + d_\omega)}.$$

$$\begin{aligned}
&= E_{(2,4)} \sum_{\theta\omega \in E(M(H_s))} \frac{H[M(H_s)]}{(d_\theta + d_\omega)} \\
&+ E_{(2,5)} \sum_{\theta\omega \in E(M(H_s))} \frac{2}{(d_\theta + d_\omega)} \\
&+ |E_{(3,5)}| \sum_{\theta\omega \in E(M(H_s))} \frac{2}{(d_\theta + d_\omega)} \\
&+ E_{(3,6)} \sum_{\theta\omega \in E(M(H_s))} \frac{2}{(d_\theta + d_\omega)} \\
&+ E_{(4,5)} \sum_{\theta\omega \in E(M(H_s))} \frac{2}{(d_\theta + d_\omega)} \\
&+ E_{(5,5)} \sum_{\theta\omega \in E(M(H_s))} \frac{2}{(d_\theta + d_\omega)} \\
&+ E_{(5,6)} \sum_{\theta\omega \in E(M(H_s))} \frac{2}{(d_\theta + d_\omega)} \\
&+ E_{(6,6)} \sum_{\theta\omega \in E(M(H_s))} \frac{2}{(d_\theta + d_\omega)}
\end{aligned}$$

$$\begin{aligned}
H[M(H_s)] &= \frac{24}{6} + 12(s-1)\frac{2}{7} + 12(s-1)\frac{2}{8} \\
&+ (18s^2 - 30s + 12)\frac{2}{9} \\
&+ (12)\frac{2}{9} + 6(2s-3)\frac{2}{10} \\
&+ 12(s-1)\frac{2}{11} + 18(s^2 - 2s \\
&+ 1)\frac{2}{12}.
\end{aligned}$$

$$\begin{aligned}
H[M(H_s)] &= (s-1)\frac{24}{7} + 3(s-1) + (6s^2 \\
&- 10s + 4)\frac{2}{3} + (2s-3)\frac{6}{5} + (s-1)\frac{24}{11} \\
&+ 3(s^2 - 2s + 1)\frac{20}{3}.
\end{aligned}$$

$$H[M(H_s)] = \frac{1913}{1155}s + \frac{142}{1155} + 7s^2.$$

$$M_1(G) = \sum_{\theta\omega \in E(G)} (d_\theta + d_\omega).$$

$$\begin{aligned}
M_1[M(H_s)] &= E_{(2,4)} \sum_{\theta\omega \in E(M(H_s))} (d_\theta + d_\omega) \\
&+ E_{(2,5)} \sum_{\theta\omega \in E(M(H_s))} (d_\theta + d_\omega) \\
&+ E_{(3,5)} \sum_{\theta\omega \in E(M(H_s))} (d_\theta + d_\omega) \\
&+ E_{(3,6)} \sum_{\theta\omega \in E(M(H_s))} (d_\theta + d_\omega) \\
&+ E_{(4,5)} \sum_{\theta\omega \in E(M(H_s))} (d_\theta + d_\omega) \\
&+ E_{(5,5)} \sum_{\theta\omega \in E(M(H_s))} (d_\theta + d_\omega) \\
&+ E_{(5,6)} \sum_{\theta\omega \in E(M(H_s))} (d_\theta + d_\omega) \\
&+ E_{(6,6)} \sum_{\theta\omega \in E(M(H_s))} (d_\theta + d_\omega) \\
M_1[M(H_s)] &= 72 + 12(s-1)7 + 12(s-1)8 \\
&+ (18s^2 - 30s + 12)9 + 108 \\
&+ 6(2s-3)10 + 12(s-1)11 \\
&+ 18(s^2 - 2s + 1)12 \\
M_1[M(H_s)] &= 432s + 27(6s^2 - 10s + 4) \\
&+ 216(s^2 - 2s + 1) - 312. \\
M_1[M(H_s)] &= 378s^2 - 270s + 12. \\
M_2(G) &= \sum_{\theta\omega \in E(G)} (d_\theta d_\omega).
\end{aligned}$$

$$\begin{aligned}
M_2[M(H_s)] &= E_{(2,4)} \sum_{\theta\omega \in E(M(H_s))} (d_\theta d_\omega) \\
&+ E_{(2,5)} \sum_{\theta\omega \in E(M(H_s))} (d_\theta d_\omega) \\
&+ E_{(3,5)} \sum_{\theta\omega \in E(M(H_s))} (d_\theta d_\omega) \\
&+ E_{(3,6)} \sum_{\theta\omega \in E(M(H_s))} (d_\theta d_\omega) \\
&+ E_{(4,5)} \sum_{\theta\omega \in E(M(H_s))} (d_\theta d_\omega) \\
&+ E_{(5,5)} \sum_{\theta\omega \in E(M(H_s))} (d_\theta d_\omega) \\
&+ E_{(5,6)} \sum_{\theta\omega \in E(M(H_s))} (d_\theta d_\omega) \\
&+ E_{(6,6)} \sum_{\theta\omega \in E(M(H_s))} (d_\theta d_\omega). \\
M_2[M(H_s)] &= (12)8 + 12(s-1)10 + 12(s-1)15 \\
&+ (18s^2 - 30s - 1)18 + (12)20 + 6(2s-3)25 \\
&+ 12(s-1)30 + 18(s^2 - 2s + 1)36. \\
M_2[M(H_s)] &= 960s + 54(6s^2 - 10s + 4) \\
&+ 648(s^2 - 2s + 1) - 774. \\
M_2[M(H_s)] &= 972s^2 - 876s + 90.
\end{aligned}$$

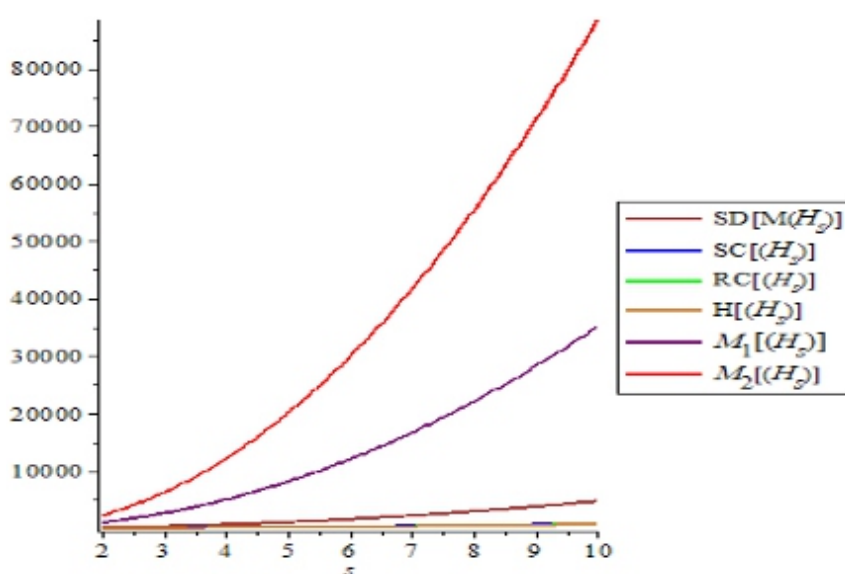


FIGURE 6 Graphical representation of middle graph of (HS)

Comparison

In this section, we provide the comparison of the above-computed topological indices numerically and the graphically. The numerical comparison of $M(H_s)$ where, $s = 2, 3, \dots, 10$, as presented in Table 4, and the graphical comparison is displayed in the Figure 6.

TABLE 4 Numerical results of middle graph of (H_s)

s	$SD[M(H_s)]$	$SC[M(H_s)]$	$RC[M(H_s)]$	$H[M(H_s)]$	$M_1[M(H_s)]$	$M_2[M(H_s)]$
2	129.6	32.192	24.475	24.810	984	2226
3	324.6	71.383	57.510	58.154	2604	6210
4	627.6	124.57	105.03	105.50	4980	12138
5	1038.6	191.76	167.03	166.84	8112	20010
6	1557.6	272.96	243.52	242.19	12000	29825
7	2184.6	368.15	334.50	331.53	16644	41586
8	2919.6	477.35	439.96	434.87	22044	55290
9	3762.6	600.52	559.91	552.22	28200	70938
10	4713.6	737.72	694.34	683.56	35112	88530

Conclusion

Topological indices help to understand the information about biological activity, chemical reactivity, and physical characteristics of chemical compounds. We derived the general formulas of some of the topological indices based on the degree of vertex i.e. sum connectivity index (SC), Randic connectivity index (RC), Symmetric division degree index (SD), Harmonic index (H), and the second Zagreb index (M_2) of the middle graph of Jahangir graph. These outcomes can be employed to further understand the topological characteristics of graphs. The comparison of attained analytical expressions is expressed graphically and numerically.

Acknowledgments

The authors would like to thank the reviewers for their helpful suggestions and comments.

Conflict of Interest

The authors declare that there is no of interests regarding the publication of this manuscript.

Orcid:

Muhammad Shoaib Sardar: <https://www.orcid.org/0000-0001-7146-5639>

Muhammad Asad Ali: <https://www.orcid.org/0000-0002-9555-7885>

Murat Cancan: <https://www.orcid.org/0000-0002-8606-2274>

References

[1] R.J. Wilson, *Introduction to graph theory*, New York: John Wiley and Sons, 1986. [Google Scholar], [PDF]

- [2] M. Alaeiyan, M.S. Sardar, S. Zafar, Z. Zahid, *Int. J. Appl. Math. Machine Learning*, 2018, 8, 91-107. [Crossref], [Google Scholar], [PDF]
- [3] H. Wiener, *J. Am. Chem. Soc.*, 1947, 69, 1720. [Crossref], [Google Scholar], [Publisher]
- [4] A. Ali, S. Elumalai, T. Mansour, *MATCH Commun. Math. Comput. Chem.*, 2020, 83, 205-220. [Google Scholar], [PDF]
- [5] B. Lucic, S. Nikolic, N. Trinajstić, Ed., *Novel Molecular Structure Descriptors-Theory and Applications I*, University of Kragujevac, Kragujevac, 2020, 4, 101-136. [Google Scholar], [Publisher]
- [6] I. Gutman, B. Furtula, V. Katanic, *AKCE Int. J. Graphs Comb.*, 2018, 15, 307-312. [Crossref], [Google Scholar], [Publisher]
- [7] M.R. Farahani, *Int. J. Nanosci. Nanotechnol.*, 2012, 8, 175-180. [Pdf], [Google Scholar], [Publisher]
- [8] J. Li, W.C. Shiu, *Rocky Mountain J. Math.*, 2014, 44, 1607-1620. [Crossref], [Google Scholar], [Publisher]
- [9] M.A. Ali, M.S. Sardar, I. Siddique, D. Alrowaili, *J. Chemistry*, 2021, 2021, Article 7057412. [Crossref], [Google Scholar], [Publisher]
- [10] M. Eliasi, A. Iranmanesh, I. Gutman, *MATCH Commun. Math. Comput. Chem.*, 2012, 68, 217-230. [Google Scholar], [PDF]
- [11] M.S. Sardar, I. Siddique, D. Alrowaili, M. A. Ali, S. Akhtar, *J. Math.*, 2022. [Crossref], [Google Scholar],
- [12] M. Danish, M.A. Ali, M.W. Tasleem, S.R. Rajpoot, S. Tasleem, M. Shahzad, *Int. J. Res. Rev.*, 2021, 2, 531-541. [Pdf], [Google Scholar], [Publisher]
- [13] M.S. Sardar, I. Siddique, F. Jarad, M. A. E.M. Turkan, M. Danish, *J. Math.*, 2022. [Crossref], [Google Scholar], [Publisher]
- [14] D.A. Mojdeh, A.N. Ghameshlou, *Int. J. Contemp. Math, Sciences*, 2007, 2, 1193-1199. [Pdf], [Google Scholar], [Publisher]
- [15] Y. Gao, M.R. Farahani, W. Nazeer, *Chem. Meth.*, 2018, 2, 39-46. [Crossref], [Google Scholar], [Publisher]
- [16] S.S. Shirkol, P.P. Kumbargoudra, M.M. Kaliwal, *J. Shanghai Jiaotong University*, 2021, 17, 10-18. [Google Scholar], [PDF]
- [17] D. Afzal, S. Hussain, M. Aldemir, M. Farahani, F. Afzal, *Eurasian Chem. Commun.*, 2020, 2, 1117-1125. [Crossref], [Google Scholar], [Publisher]
- [18] S. Hussain, F. Afzal, D. Afzal, M. Farahani, M. Cancan, S. Ediz, *Eurasian Chem. Commun.*, 2021, 3, 180-186. [Crossref], [Google Scholar], [Publisher]
- [19] D.Y. Shin, S. Hussain, F. Afzal, C. Park, D. Afzal, M.R. Farahani. *Frontier Chem.*, 2021, 8, 613873-61380. [Crossref], [Google Scholar], [Publisher]
- [20] W. Gao, M.R. Farahani, S. Wang, M.N. Husin, *Appl. Math. Comput.*, 2017, 308, 11-17. [Crossref], [Google Scholar], [Publisher]
- [21] H. Wang, J.B. Liu, S. Wang, W. Gao, S. Akhter, M. Imran, M.R. Farahani, *Discrete Dyn. Nat. Soc.*, 2017, 2017, Article ID 2941615. [Crossref], [Google Scholar],
- [22] W. Gao, M.K. Jamil, A. Javed, M.R. Farahani, M. Imran. *UPB Sci. Bulletin B.*, 80, 97-104, 2018. [Google Scholar], [Publisher]
- [23] S. Akhter, M. Imran, W. Gao, M.R. Farahani, *Hacet. J. Math. Stat.*, 2018, 47, 1935. [Crossref], [Google Scholar], [Publisher]

- [24] X. Zhang, X. Wu, S. Akhter, M.K. Jamil, J.B. Liu, M.R. Farahani, *Symmetry*, 2018, 10, 751. [Crossref], [Google Scholar], [Publisher]
- [25] H. Yang, A.Q. Baig, W. Khalid, M.R. Farahani, X. Zhang, *J. Chem.*, 2019. [Crossref], [Google Scholar], [Publisher]
- [26] L Yan, M.R. Farahani, W. Gao, *Open J. Math. Sci.*, 2018, 2, 323-337. [Crossref], [Google Scholar], [Publisher]
- [27] M. Imran, M.K. Siddiqui, S. Ahmad, M.F. Hanif, MH Muhammad, M.R. Farahani, *J. Discret. Math. Sci. Cryptogr.*, 2018, 22, 12291248. [Crossref], [Google Scholar], [Publisher]
- [28] S. Ahmad, H.M.A. Siddiqui, A Ali, M.R. Farahani, M. Imran, I.N. Cangul, *On J. Discret. Math. Sci. Cryptogr.*, 2019, 22, 1151-1164. [Crossref], [Google Scholar], [Publisher]
- [29] Z. Shao, A.R. Virk, M.S. Javed, M.A. Rehman, M.R. Farahani, *Eng. Appl. Sci. Lett.*, 2019, 2, 01-11. [Crossref], [Google Scholar], [Publisher]
- [30] M. Cancan, S Ediz, M Alaeiyan, M.R. Farahani, *J. Inf. Opt. Sci.*, 2020, 41, 949-957. [Crossref], [Google Scholar], [Publisher]
- [31] M. Cancan, S Ediz, M.R. Farahani, M.R. Farahani, *Eurasian Chem. Commun.*, 2020, 2, 641-645. [Crossref],
- [32] M. Alaeiyan, [Google C. Scholar], Natarajan, G. Sathiamoorthy, M.R. Farahani, *Eurasian Chem. Commun.*, 2020, 2, 646-651. [Crossref], [Google Scholar], [Publisher]
- [33] M. Alaeiyan, F. Afzal, M.R. Farahani, MA Rostami, *J. Inf. Opt. Sci.*, 2020, 41, 933-939. [Crossref], [Google Scholar], [Publisher]
- [34] M. Cancan, S. Ediz, S. Fareed, M.R. Farahani, *J. Inf. Opt. Sci.*, 2020, 41, 925-932. [Crossref], [Google Scholar], [Publisher]
- [35] D. Afzal, S. Ali, F. Afzal, M. Cancan, S. Ediz, M.R. Farahani, *J. Discret. Math. Sci. Cryptogr.*, 2021, 24, 427-438. [Crossref], [Google Scholar], [Publisher]
- [36] Z. Mokhayeri, *Adv. J. Chem.*, 2022, 4, 104112. [Crossref], [Publisher]
- [37] B. Baghernejad, N.S. Soltani, *Asian J. Green Chem.*, 2022, 6, 166-174. [Crossref], [Publisher]
- [38] E.S. Whaib, M.A. Mousa, *Chem. Methodol.*, 2022, 783-789. [Crossref], [Pdf], [Publisher]
- [39] N. Farhami, *J. Appl. Organomet. Chem.*, 2022, 2, 163-172. [Crossref], [Pdf], [Publisher]
- [40] M. Jafari, *Prog. Chem. and Biochem. Res.*, 2022, 5, 115-124. [Crossref], [Google Scholar], [Publisher]

Instructions for Authors

Essentials for Publishing in this Journal

- 1 Submitted articles should not have been previously published or be currently under consideration for publication elsewhere.
- 2 Conference papers may only be submitted if the paper has been completely re-written (taken to mean more than 50%) and the author has cleared any necessary permission with the copyright owner if it has been previously copyrighted.
- 3 All our articles are refereed through a double-blind process.
- 4 All authors must declare they have read and agreed to the content of the submitted article and must sign a declaration correspond to the originality of the article.

Submission Process

All articles for this journal must be submitted using our online submissions system. <http://enrichedpub.com/> . Please use the Submit Your Article link in the Author Service area.

Manuscript Guidelines

The instructions to authors about the article preparation for publication in the Manuscripts are submitted online, through the e-Ur (Electronic editing) system, developed by **Enriched Publications Pvt. Ltd.** The article should contain the abstract with keywords, introduction, body, conclusion, references and the summary in English language (without heading and subheading enumeration). The article length should not exceed 16 pages of A4 paper format.

Title

The title should be informative. It is in both Journal's and author's best interest to use terms suitable. For indexing and word search. If there are no such terms in the title, the author is strongly advised to add a subtitle. The title should be given in English as well. The titles precede the abstract and the summary in an appropriate language.

Letterhead Title

The letterhead title is given at a top of each page for easier identification of article copies in an Electronic form in particular. It contains the author's surname and first name initial, article title, journal title and collation (year, volume, and issue, first and last page). The journal and article titles can be given in a shortened form.

Author's Name

Full name(s) of author(s) should be used. It is advisable to give the middle initial. Names are given in their original form.

Contact Details

The postal address or the e-mail address of the author (usually of the first one if there are more Authors) is given in the footnote at the bottom of the first page.

Type of Articles

Classification of articles is a duty of the editorial staff and is of special importance. Referees and the members of the editorial staff, or section editors, can propose a category, but the editor-in-chief has the sole responsibility for their classification. Journal articles are classified as follows:

Scientific articles:

1. Original scientific paper (giving the previously unpublished results of the author's own research based on management methods).
2. Survey paper (giving an original, detailed and critical view of a research problem or an area to which the author has made a contribution visible through his self-citation);
3. Short or preliminary communication (original management paper of full format but of a smaller extent or of a preliminary character);
4. Scientific critique or forum (discussion on a particular scientific topic, based exclusively on management argumentation) and commentaries. Exceptionally, in particular areas, a scientific paper in the Journal can be in a form of a monograph or a critical edition of scientific data (historical, archival, lexicographic, bibliographic, data survey, etc.) which were unknown or hardly accessible for scientific research.

Professional articles:

1. Professional paper (contribution offering experience useful for improvement of professional practice but not necessarily based on scientific methods);
2. Informative contribution (editorial, commentary, etc.);
3. Review (of a book, software, case study, scientific event, etc.)

Language

The article should be in English. The grammar and style of the article should be of good quality. The systematized text should be without abbreviations (except standard ones). All measurements must be in SI units. The sequence of formulae is denoted in Arabic numerals in parentheses on the right-hand side.

Abstract and Summary

An abstract is a concise informative presentation of the article content for fast and accurate Evaluation of its relevance. It is both in the Editorial Office's and the author's best interest for an abstract to contain terms often used for indexing and article search. The abstract describes the purpose of the study and the methods, outlines the findings and state the conclusions. A 100- to 250-Word abstract should be placed between the title and the keywords with the body text to follow. Besides an abstract are advised to have a summary in English, at the end of the article, after the Reference list. The summary should be structured and long up to 1/10 of the article length (it is more extensive than the abstract).

Keywords

Keywords are terms or phrases showing adequately the article content for indexing and search purposes. They should be allocated heaving in mind widely accepted international sources (index, dictionary or thesaurus), such as the Web of Science keyword list for science in general. The higher their usage frequency is the better. Up to 10 keywords immediately follow the abstract and the summary, in respective languages.

Acknowledgements

The name and the number of the project or programmed within which the article was realized is given in a separate note at the bottom of the first page together with the name of the institution which financially supported the project or programmed.

Tables and Illustrations

All the captions should be in the original language as well as in English, together with the texts in illustrations if possible. Tables are typed in the same style as the text and are denoted by numerals at the top. Photographs and drawings, placed appropriately in the text, should be clear, precise and suitable for reproduction. Drawings should be created in Word or Corel.

Citation in the Text

Citation in the text must be uniform. When citing references in the text, use the reference number set in square brackets from the Reference list at the end of the article.

Footnotes

Footnotes are given at the bottom of the page with the text they refer to. They can contain less relevant details, additional explanations or used sources (e.g. scientific material, manuals). They cannot replace the cited literature.

The article should be accompanied with a cover letter with the information about the author(s): surname, middle initial, first name, and citizen personal number, rank, title, e-mail address, and affiliation address, home address including municipality, phone number in the office and at home (or a mobile phone number). The cover letter should state the type of the article and tell which illustrations are original and which are not.